TECHNICAL REPORT HL-90-20

US Army Corps of Engineers

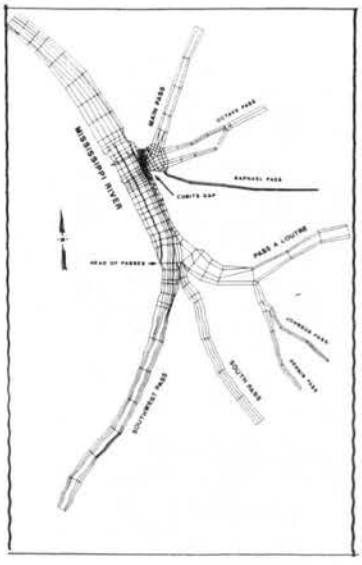

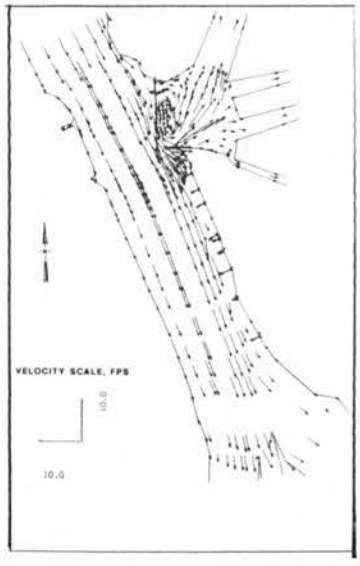

HYDRAULICS LABORATORY

DREDGING ALTERNATIVES STUDY CUBITS GAP, LOWER MISSISSIPPI RIVER

Report 2
TABS-2 NUMERICAL MODEL INVESTIGATION

VOLUME I
MAIN TEXT AND APPENDIX A

by

H. J. Lin, W. D. Martin, D. R. Richards

Hydraulics Laboratory

DEPARTMENT OF THE ARMY
Waterways Experiment Station, Corps of Engineers
3909 Halls Ferry Road, Vicksburg, Mississippi 39180-6199

November 1990
Report 2 of a Series

Approved For Public Release; Distribution Unlimited

Prepared for US Army Engineer District, New Orleans
New Orleans, Louisiana 70160-0267

Destroy this report when no longer needed. Do not return it to the originator.

The findings in this report are not to be construed as an official Department of the Army position unless so designated by other authorized documents.

The contents of this report are not to be used for advertising, publication, or promotional purposes. Citation of trade names does not constitute an official endorsement or approval of the use of such commercial products.

REPORT DOCUMENTATION PAGE

Form Approved
OMB No. 0704-0188

1. AGENCY USE ONLY (Leave blank)	2. REPORT DATE	3. REPORT TYPE AND DATES COVERED
	November 1990	Report 2 of a series

4. TITLE AND SUBTITLE

Dredging Alternatives Study, Cubits Gap, Lower Mississippi River; TABS-2 Numerical Model Investigation

5. FUNDING NUMBERS

6. AUTHOR(S)

Lin, H. J.; Martin, W. D.; and Richards, D. R.

7. PERFORMING ORGANIZATION NAME(S) AND ADDRESS(ES)

USAE Waterways Experiment Station
Hydraulics Laboratory
3909 Halls Ferry Road
Vicksburg, MS 39180-6199

8. PERFORMING ORGANIZATION REPORT NUMBER

Technical Report
HL-90-20

9. SPONSORING/MONITORING AGENCY NAME(S) AND ADDRESS(ES)

USAED, New Orleans, PO Box 60267,
New Orleans, LA 70160-0267

10. SPONSORING/MONITORING AGENCY REPORT NUMBER

11. SUPPLEMENTARY NOTES

A limited number of copies of Appendix B were published under separate cover. Copies of this report and Appendix B are available from National Technical Information Service, 5285 Port Royal Road, Springfield, VA 22161.

12a. DISTRIBUTION/AVAILABILITY STATEMENT

Approved for public release; distribution unlimited

12b. DISTRIBUTION CODE

13. ABSTRACT *(Maximum 200 words)*

This report presents results from the numerical model investigation whose primary objective was to determine the best method to control shoaling in the navigation channel between Cubits Gap and Head of Passes. The secondary objective was to evaluate the best design configuration for a structural dike plan located at Cubits Gap and the ability of these designs to return the flow distribution to its historical levels.

Several plans were proposed by the US Army Engineer District, New Orleans, and local shipping interests to alleviate the recurrence of these shoaling conditions. They included a sediment trap, advance maintenance, and additional training structures. The first two addressed shoaling problems in the reach between Cubits Gap and Head of Passes. The latter addressed shoaling and flow distribution in Cubits Gap.

This investigation used the TABS-2 finite element numerical model RMA-2V for hydrodynamic analysis and STUDH for sediment transport conputation. A large-flow 87-day hydrograph was used to determine the performance of each plan.

14. SUBJECT TERMS		15. NUMBER OF PAGES
Dike	Sediment trap	Vol I,56;Vol II,26
Hydrodynamic	Sedimentation	16. PRICE CODE
Numerical model		

17. SECURITY CLASSIFICATION OF REPORT	18. SECURITY CLASSIFICATION OF THIS PAGE	19. SECURITY CLASSIFICATION OF ABSTRACT	20. LIMITATION OF ABSTRACT
Unclassified	Unclassified		

13. (Concluded).

Results from the sedimentation modeling showed that the best nonstructural plan was advance maintenance. It provided a smaller quantity of shoaling than the sediment trap plan and affected a smaller area of the navigation channel. Both nonstructural plans, however, would increase the channel shoaling rate compared to existing conditions. For the structural plan, Plan 1 with a 2,800-ft-long angle dike and 800-ft-long headland dike provided the least amount of shoaling of any plan tested. All three dike plans tested would result in a substantial reduction in channel shoaling. Results from the hydrodynamic modeling showed that dike plan 1 returned the flow distribution at Cubits Gap to the amount expected with the supplement II works in place. This study did not address long-term sedimentation effects within Cubits Gap. If one of the structural plans is selected for implementation, a detailed study in the vicinity of Cubits Gap is recommended to optimize the performance of the structure.

PREFACE

The two-dimensional hydrodynamic and sediment study of Cubits Gap on the Lower Mississippi River, reported herein, was conducted at the US Army Engineer Waterways Experiment Station (WES), Vicksburg, MS, at the request of the US Army Engineer District, New Orleans (LMN). This is Report 2 of two reports. Report 1 describes a numerical model investigation of dredging alternatives for Cubits Gap.

This investigation was conducted during the period August 1989 to February 1990 by personnel of the Hydraulics Laboratory at WES under the direction of Messrs. F. A. Herrmann, Jr., Chief of the Hydraulics Laboratory; R. A. Sager, Assistant Chief of the Hydraulics Laboratory; and W. H. McAnally, Jr., Chief of the Estuaries Division (ED), Hydraulics Laboratory. The study was conducted and this report prepared by Dr. H. J. Lin, Estuarine Engineering Branch (EEB), ED; Mr. W. D. Martin, Chief, EEB; and Mr. D. R. Richards, Estuarine Simulation Branch, ED. This report was edited by Mrs. M. C. Gay, Information Technology Laboratory, WES.

Messrs. C. W. Soileau and Bill Garrett, LMN, provided valuable technical consultation.

Commander and Director of WES during the preparation of this report was COL Larry B. Fulton, EN. Technical Director was Dr. Robert W. Whalin.

CONTENTS

* A limited number of copies of Appendix B were published under separate cover. Copies are available from National Technical Information Service, 5285 Port Royal Road, Springfield, VA 22151 or US Army Engineer Waterways Experiment Station, ATTN: CEWES-HE-E, 3909 Halls Ferry Road, Vicksburg, MS 39180-6199.

CONVERSION FACTORS, NON-SI TO SI (METRIC)
UNITS OF MEASUREMENT

Non-SI units of measurement used in this report can be converted to SI (metric) units as follows:

Multiply	By	To Obtain
acres	4,046.873	square metres
cubic feet	0.02831685	cubic metres
cubic yards	0.7645549	cubic metres
degrees (angle)	0.01745329	radians
feet	0.3048	metres
miles (US statute)	1.609347	kilometres
pounds (force)-second per foot squared	47.88026	pascals-second

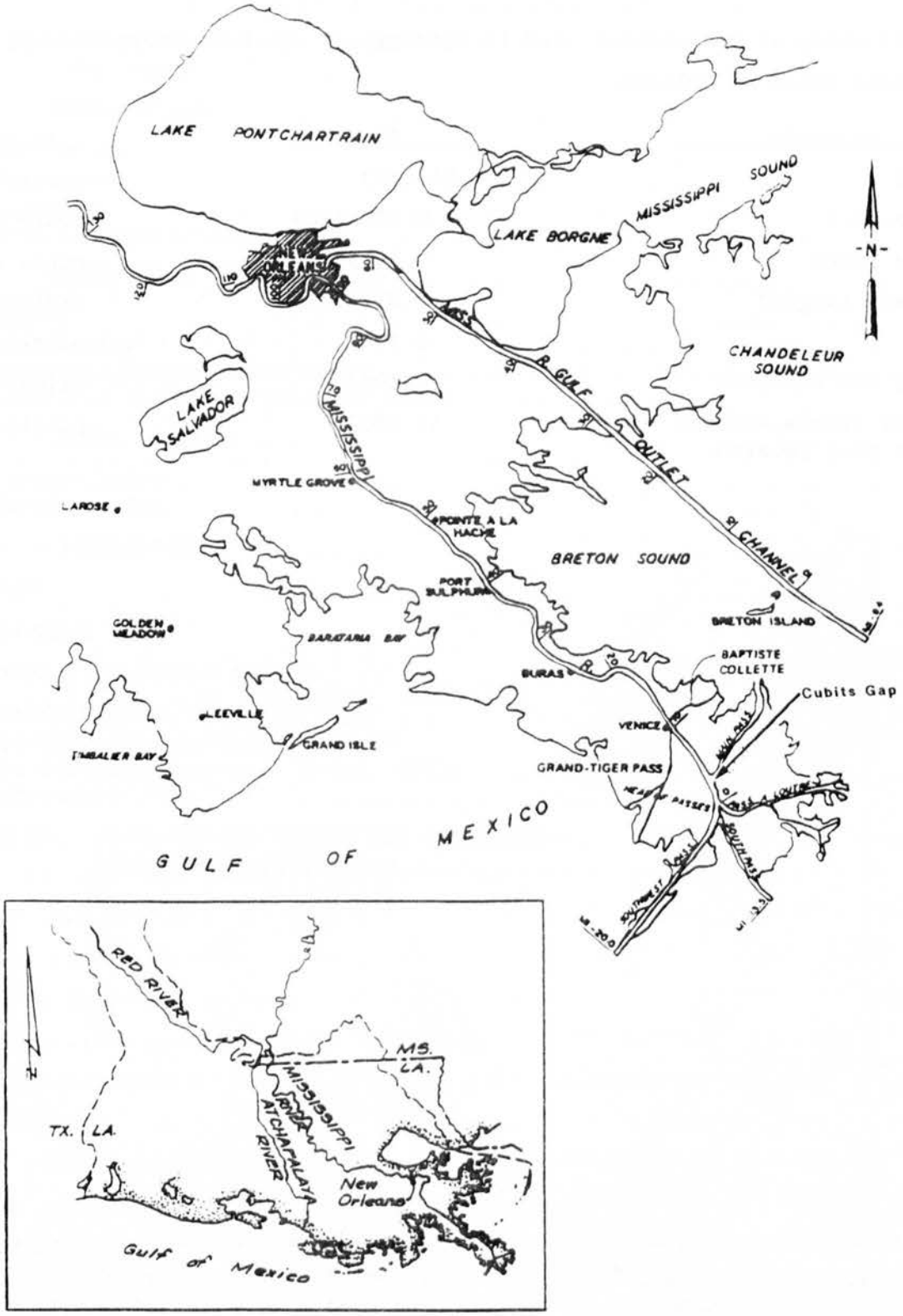

Figure 1. Location map

DREDGING ALTERNATIVES STUDY

CUBITS GAP, LOWER MISSISSIPPI RIVER

TABS-2 NUMERICAL MODEL INVESTIGATION

PART I: INTRODUCTION

Cubits Gap

1. Cubits Gap derives its name from the Cubit family, which lived about 3 miles* above the Head of Passes (AHP) on the left descending bank of the Mississippi River before and during the Civil War. Late in the Civil War, Union forces cut through a bulkhead near the Cubit house, diverting a portion of the riverflow into a fisherman's canal. The channel enlarged and soon became a permanent distributary of the Mississippi River. River pilots called the new channel Cubits Gap (Bragg 1977). The present-day location of the gap at mile 3.5 AHP is shown in Figure 1.

2. In recent years, the gap has carried approximately 10 percent of the riverflow as measured at Venice, LA, located at mile 10.8 AHP. Measurements made during the spring of 1989 indicated that this percentage had risen to about 20 percent. Additionally, severe shoaling occurred just below the gap, resulting in the grounding of a Soviet vessel, the *Marshal Koniev*, and severely disrupting navigation for a period of weeks.

3. Several plans were proposed by the US Army Engineer District, New Orleans, and local shipping interests to alleviate the recurrence of this shoaling condition, including a sediment trap, advance maintenance, and additional training structures. The first two addressed the increased shoaling in the main channel reach between Cubits Gap and Head of Passes (HP). The latter addressed both the increased shoaling and the increase in flow through Cubits Gap.

4. Channel modifications in the delta region must be carefully analyzed as all possess the potential to alter flow distributions through the various distributaries (Richards and Trawle 1988). Changes in flow distributions also

---

* A table of factors for converting non-SI units of measurement to SI (metric) units is found on page 3.

have the potential to severely aggravate shoaling in the navigation channel. With these concerns in mind, the New Orleans District asked the US Army Engineer Waterways Experiment Station (WES) to conduct large-scale numerical model studies that could quantitatively predict the hydrodynamic and sediment impacts of the various plans. The resulting effort was subdivided into one- and two-dimensional modeling efforts. The one-dimensional study is discussed in Report 1 of this series (Copeland, in preparation). This report covers the two-dimensional (2-D) study.

Objective

5. The primary objective of this study was to determine the best method to control shoaling in the navigation channel between Cubits Gap and HP. Secondary objectives were to evaluate the best design configuration for a structural dike plan located at Cubits Gap and the ability of the dikes to return the flow distribution to its historical levels.

Approach

6. The approach chosen was to use the TABS-2 numerical modeling system to evaluate the hydrodynamic and sediment transport performance of each plan and compare these to the existing or base condition. An existing numerical model mesh of the entire lower delta as shown in Figure 2 (Richards and Trawle 1987) was used to generate boundary conditions for a higher resolution inset model as shown in Figure 3. Both meshes incorporated the latest improvements for this reach of the River (US Army Engineer District, New Orleans, 1984). The inset model covered the area from 1.5 miles below Grand Pass to 2.5 miles below HP. This mesh included 11.5 miles of the main stem of the Mississippi River and Southwest Pass. The inset mesh reflected the geometric changes due to the near completion of the Supplement II channel improvement works (consisting mainly of dikes and bank stabilization works). Additional resolution was also added in the vicinity of Cubits Gap.

Modeled Geometries

7. Initially three conditions were to be evaluated against the base condition. These included advance maintenance from mile 0.0 to mile 4.0 AHP,

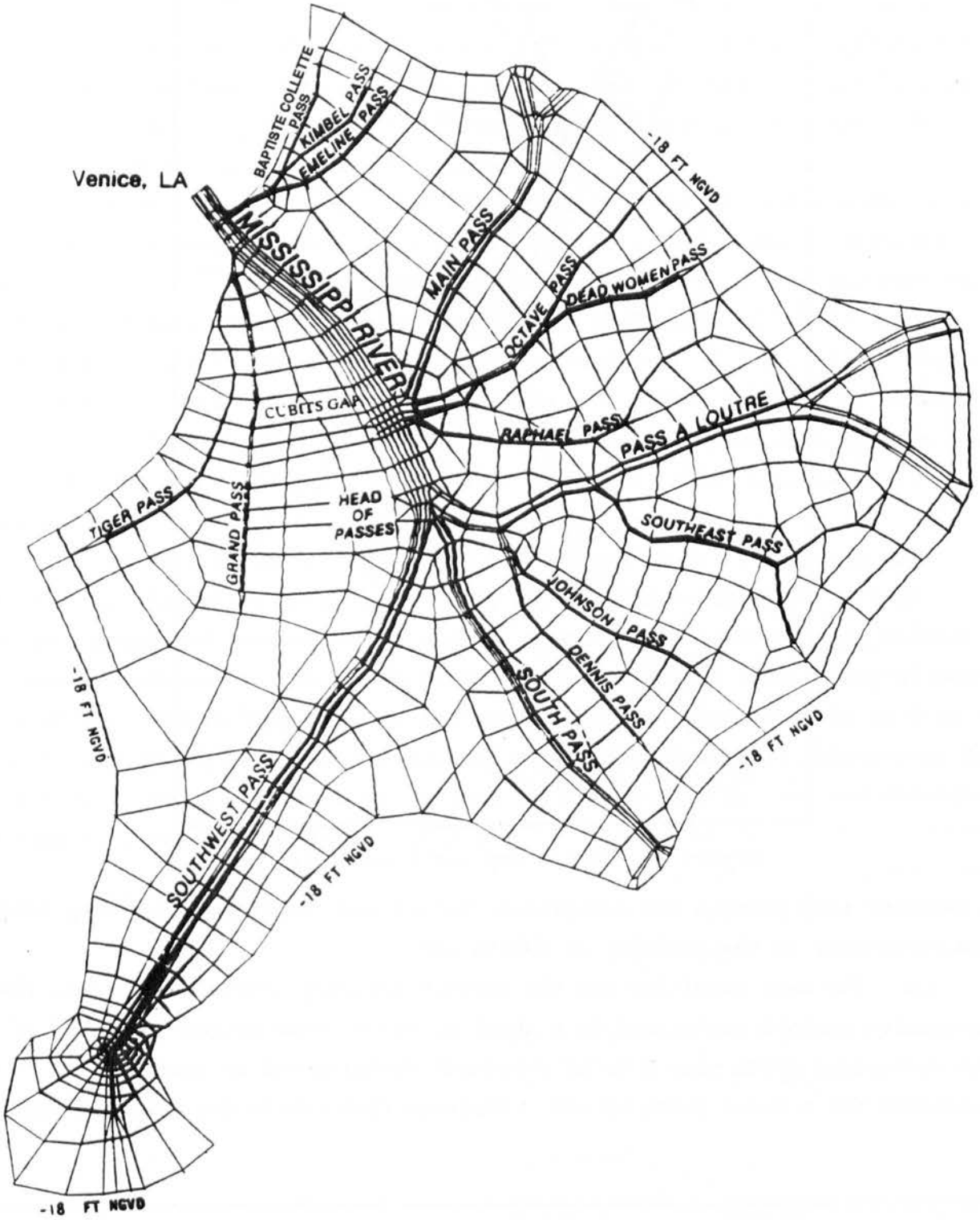

Figure 2. Full delta or global numerical mesh
(from Richards and Trawle 1987)

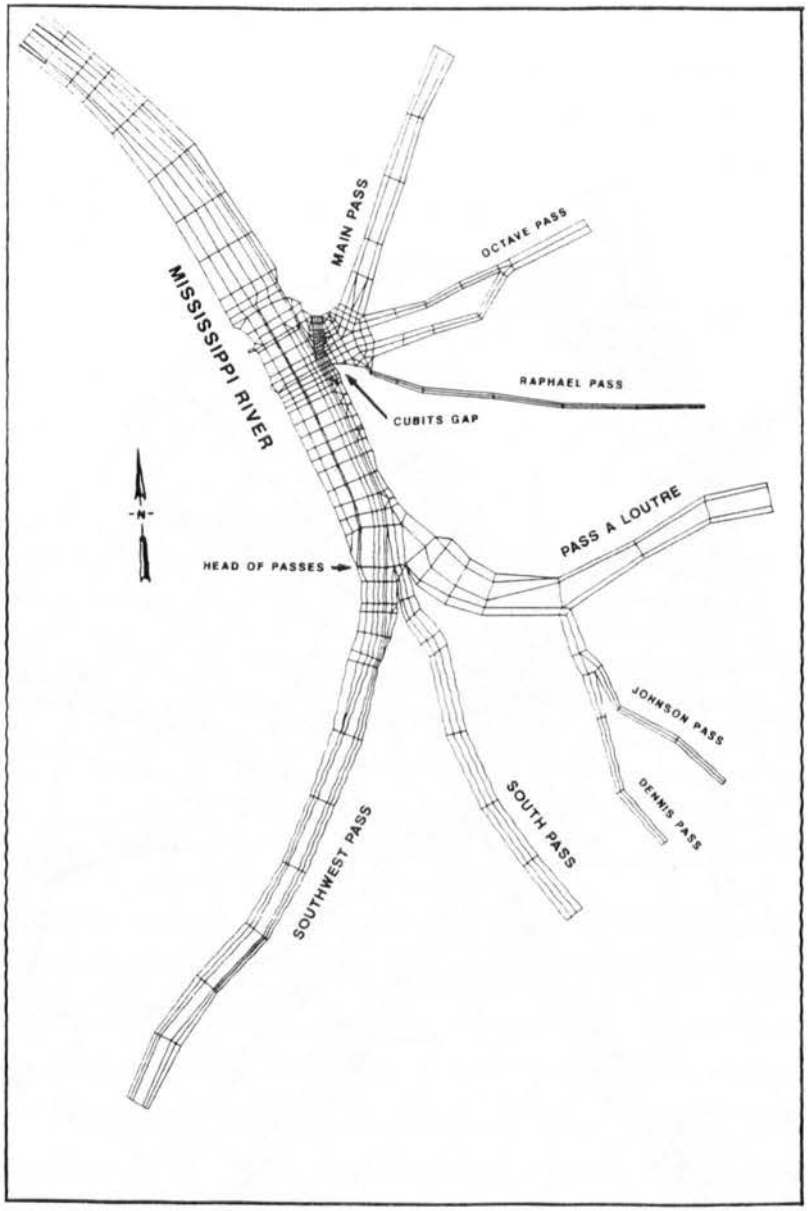

Figure 3. Cubits Gap inset numerical mesh

a sediment trap between the navigation channel and the right descending bank, and structures in the vicinity of Cubits Gap.

8. The base condition was the current dredging scheme to maintain the navigation channel authorized to a depth of -45.* This scheme consisted of the authorized depth plus 2 ft of overdepth dredging and an additional 1 ft of tolerance for a total depth of -48. Upstream from Cubits Gap, natural depths

---

* Unless otherwise noted, elevations (el) and depths are in feet referenced to the mean low Gulf (mlg) datum, which is approximately 0.78 ft below the National Geodetic Vertical Datum (NGVD).

are greater than the authorized channel depth. This condition is shown in schematic plan view in Figure 4.

9. The advance maintenance plan called for overdepth dredging to an elevation of -50. The advance maintenance extended from mile 0.0 to mile 4.0 AHP. This plan is shown in Figure 5. The sediment trap plan called for a 1,000-ft-wide sediment trap dredged to a depth of -50. The trap was located adjacent to the navigation channel between mile 0.0 and mile 4.0 AHP. This plan is shown in Figure 6.

10. After consultation with the New Orleans District, three structural configurations were chosen for the initial analysis, which was to evaluate their feasibility. All three plans featured an 800-ft-long headland structure (impermeable dike) extending upstream from the south bank of Cubits Gap. Additionally, a dike was attached to the upstream bank of Cubits Gap. Three configurations were tested with the upstream dike angled upstream at 30 deg, 45 deg, and 90 deg from a line parallel to the channel. The dike lengths were 2,800, 1,700, and 1,100 ft, respectively. These are shown schematically in Figure 7.

11. Early testing indicated that the 90- and 45-deg alignments were inferior to the 30-deg plan in that they did not reduce the flow through Cubits Gap and had less effect on channel velocities. Later testing focused on three variations to the 30-deg plan. These were the 2,800-ft-long 30-deg dike with an 800-ft-long headland structure (Figure 8), referred to as dike plan 1; the 30-deg dike with no headland structure (Figure 9), referred to as dike plan 2; and a shortened 30-deg dike (2,100 ft) with no headland structure (Figure 10), referred to as dike plan 3.

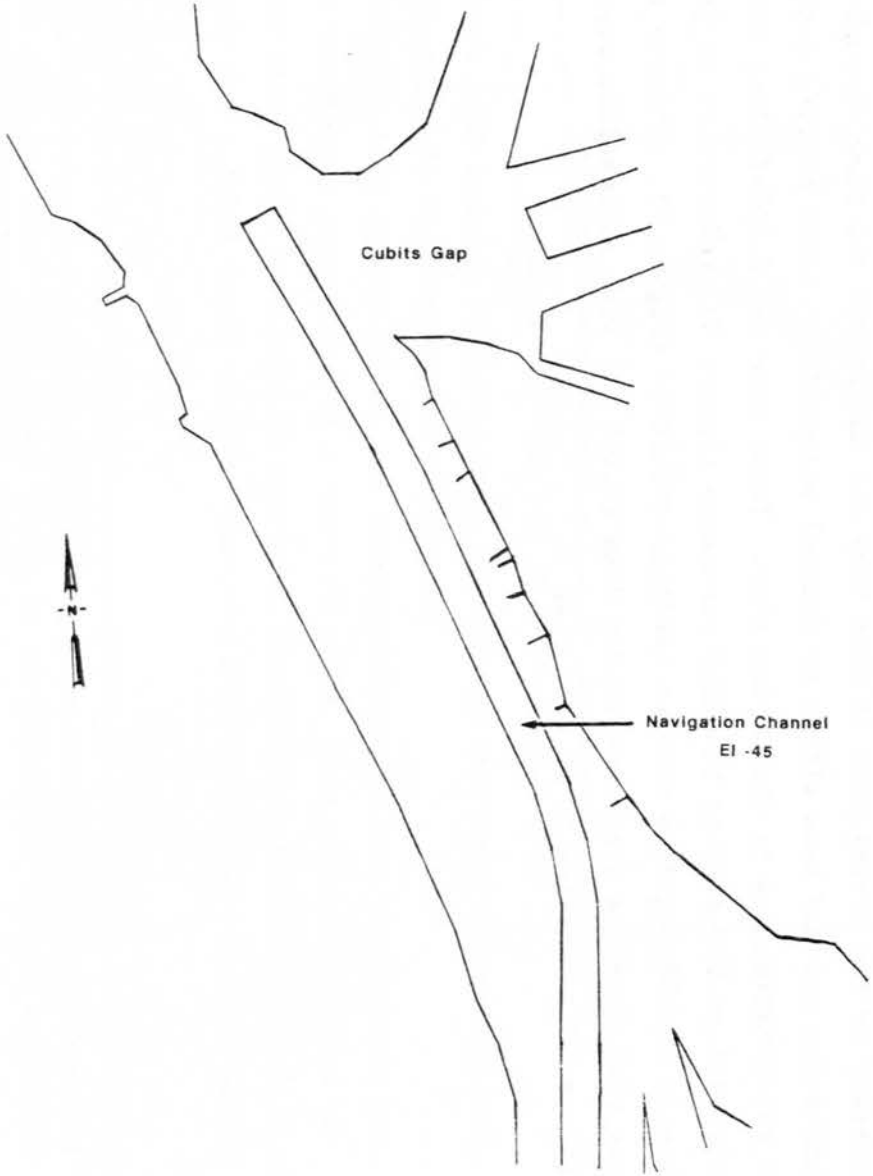

Figure 4. Existing (base) condition

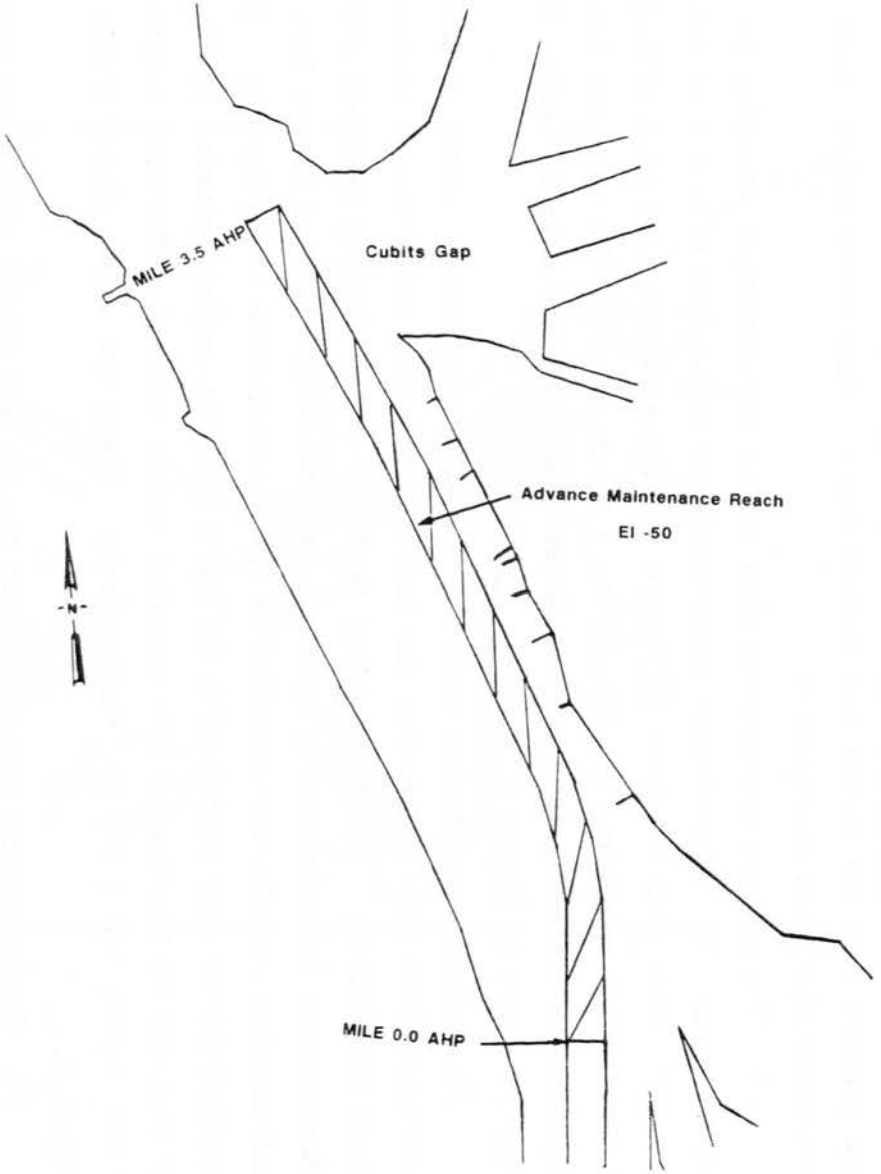

Figure 5. Advance maintenance plan

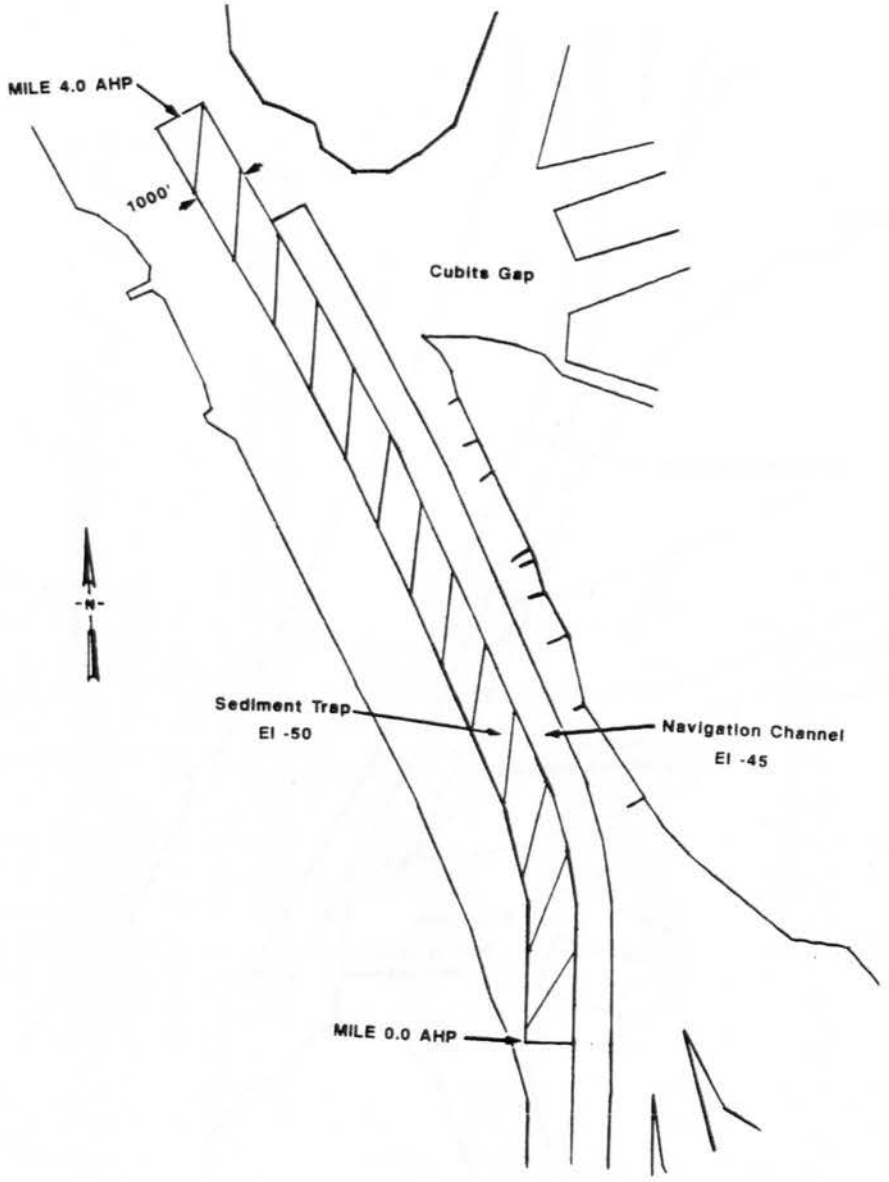

Figure 6. Sediment trap

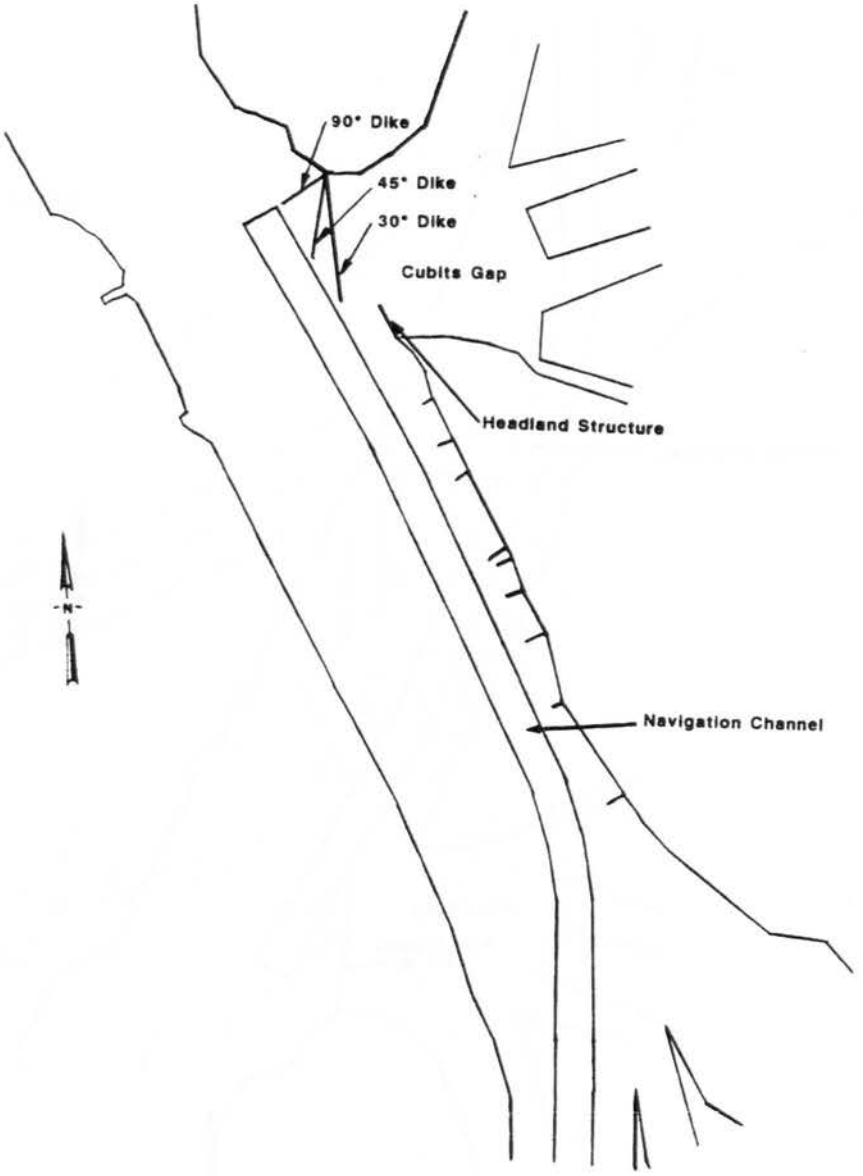

Figure 7. Three angled dikes

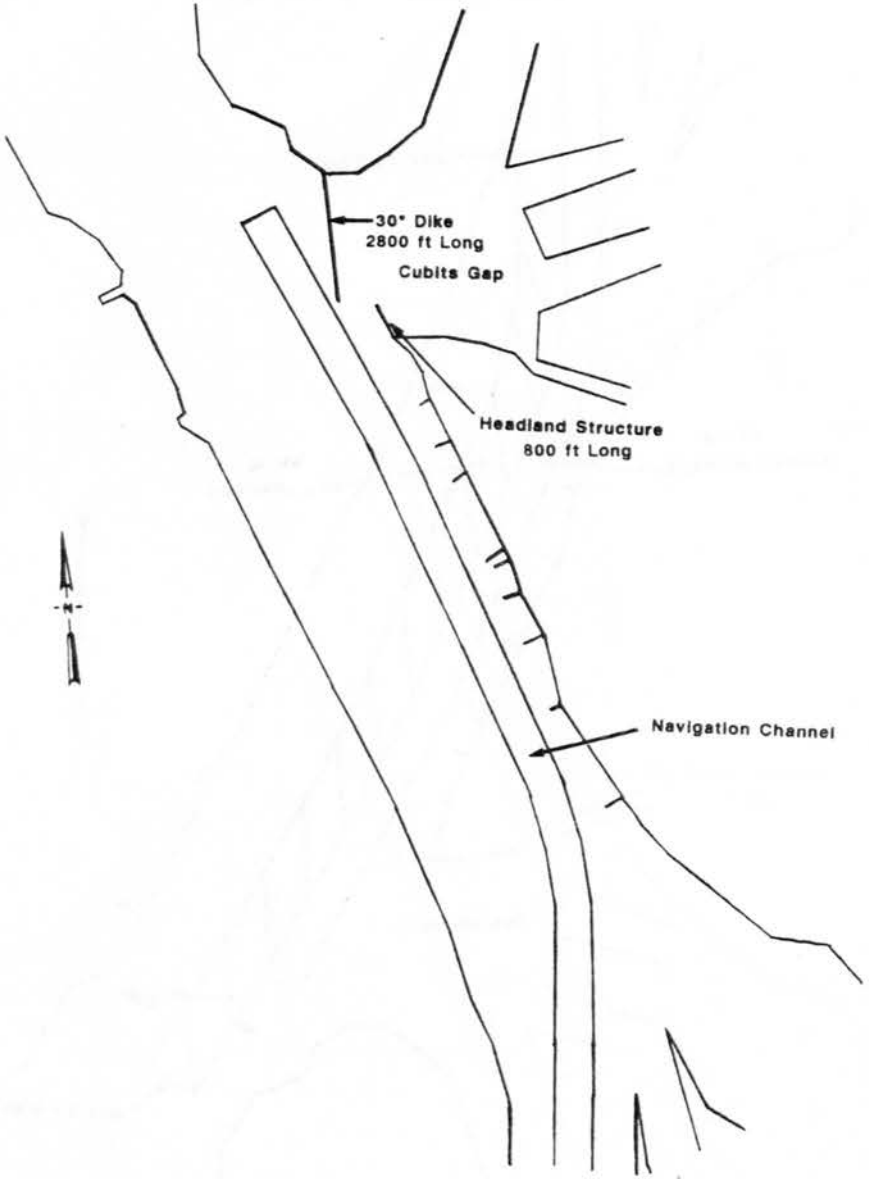

Figure 8. Dike plan 1: 30-deg dike with headland structure

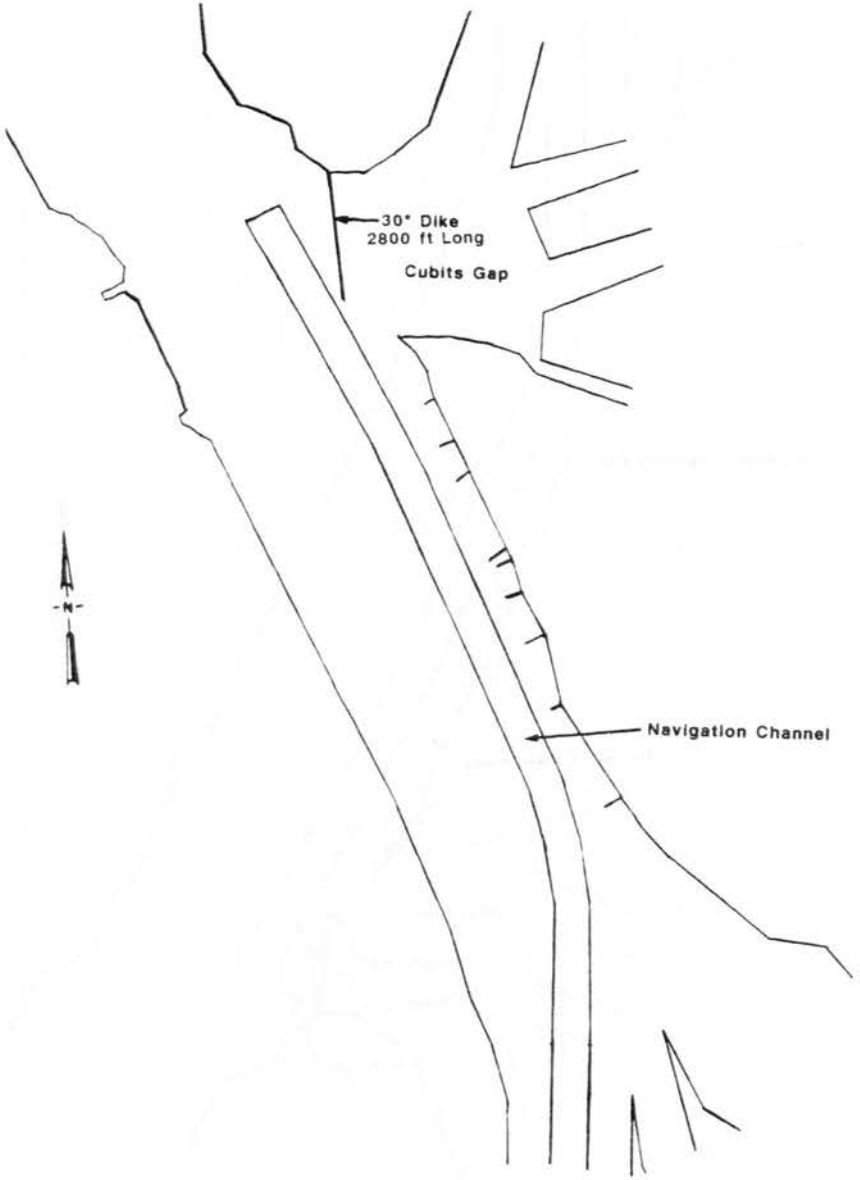

Figure 9. Dike plan 2: 30-deg dike without headland structure

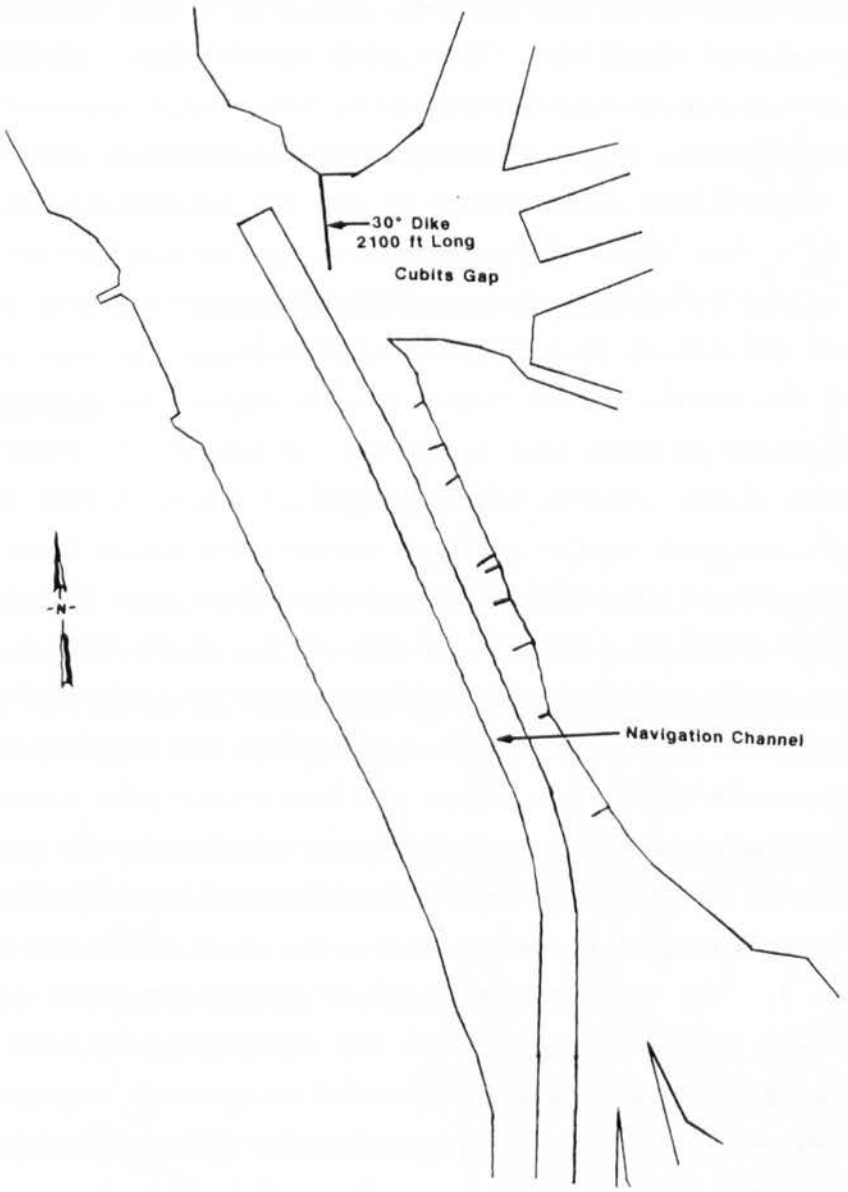

Figure 10. Dike plan 3: 30-deg dike (shortened) without headland structure

PART II: DESCRIPTION OF THE MODELS

TABS-2

12. TABS-2 is the name of a family of computer programs used in the 2-D modeling of hydrodynamics, sedimentation, and constituent transport in rivers, reservoirs, bays, and estuaries. The system was developed at WES from basic hydrodynamic and transport codes provided by Resource Management Associates, Inc., Davis, CA (Norton, King, and Orlob 1973; Ariathurai, MacArthur, and Krone 1977). Significant enhancements to the original codes have allowed for applications to a wide class of computational hydraulics problems. The system contains all of the necessary preprocessing and postprocessing utilities needed to allow relatively user-friendly applications. A more detailed description of the models in the TABS-2 system appears in Appendix A.

Mesh Design

13. The previously developed mesh of the delta area (Richards and Trawle 1987) was used to generate boundary conditions for evaluating the various plans. In this study, the delta mesh was referred to as the global mesh and is shown in Figure 2. This differentiated it from the higher resolution mesh developed to test the plans.

14. The 600-element high-resolution mesh was based on a portion of the global mesh and was developed to test the various plans. It covered the Mississippi River from just below Grand Pass to about 2 miles below HP, as shown in Figure 3. The model included all of Cubits Gap as it existed at the time the study was initiated, along with the distributaries that carry the diverted Mississippi River waters to the Gulf of Mexico. The existing condition geometry was defined by New Orleans District hydrographic survey sheets dated 3 February 1989.

15. The average channel depth as recorded on the hydrographic survey sheets was about -45. This geometry was used for verification of the numerical 2-D model to observed field hydrodynamic and sediment conditions during the period 7 February to 4 May 1989. Since the channel is normally maintained to a depth of -48 as discussed previously, the channel depths for the base

condition were redefined to -48 and this depth was used for comparison with the alternative plans.

16. The mesh was designed such that elements representing all aspects of each plan were included. Nodal elevations were then lowered or raised to those of model dikes, the sediment trap, and the deeper channel as appropriate. For the structural dike plans, the headland dike, when present, was always 800 ft long. The 30-deg dike was 2,800 ft long for dike plans 1 and 2 and 2,100 ft long for dike plan 3. In all the meshes, depths for the distributary streams were uncertain, so the previous values used by Richards and Trawle (1988) were used.

Numerical Hydrodynamic Model

Boundary conditions

17. Boundary conditions for all tests consisted of upstream velocities and downstream channel and distributary water levels. These were generated by running the global model and transferring the values from interior nodes to the high-resolution mesh exterior boundary nodes. The observed discharge hydrograph at Tarbert Landing, MS, for the 87-day period between 7 February and 4 May 1989 was provided by the New Orleans District. A discharge histogram was developed from this hydrograph that reduced the 87 days of flow to 19 discrete events that maintained the shape and volume of the original hydrograph. Both the observed and histogram hydrographs are shown in Figure 11. The histogram flows were then run through the global model to develop boundary conditions for the inset mesh. The Gulf level was held constant for all runs at an elevation corresponding to the mean Gulf level.

Verification

18. The global hydrodynamic model was reactivated and reverified prior to initiation of the actual inset mesh development (Richards and Trawle 1988). Field data were collected at Grand Pass on 1 May 1989 and at Cubits Gap on 2 May 1989 (Fagerburg, in preparation). These data were reproduced by the inset model, as indicated by matching depth-averaged velocities below Cubits Gap and in the four distributaries of Cubits Gap (Figure 12), and are shown in Figures 13-17. This reproduction was accomplished by adjusting eddy viscosity and Manning's n values and decreasing the water level at the exterior nodes of the distributaries of Cubits Gap. When this process was completed, the

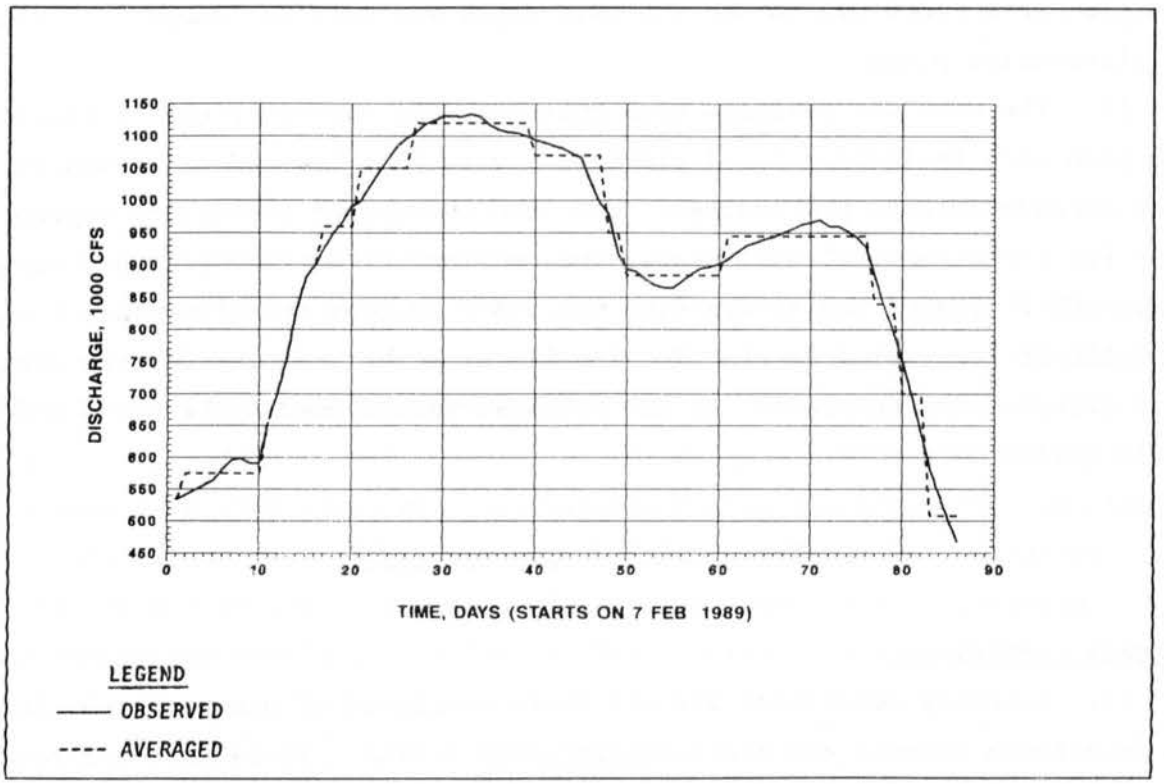

Figure 11. Observed and histogram hydrographs, Tarbert Landing, MS

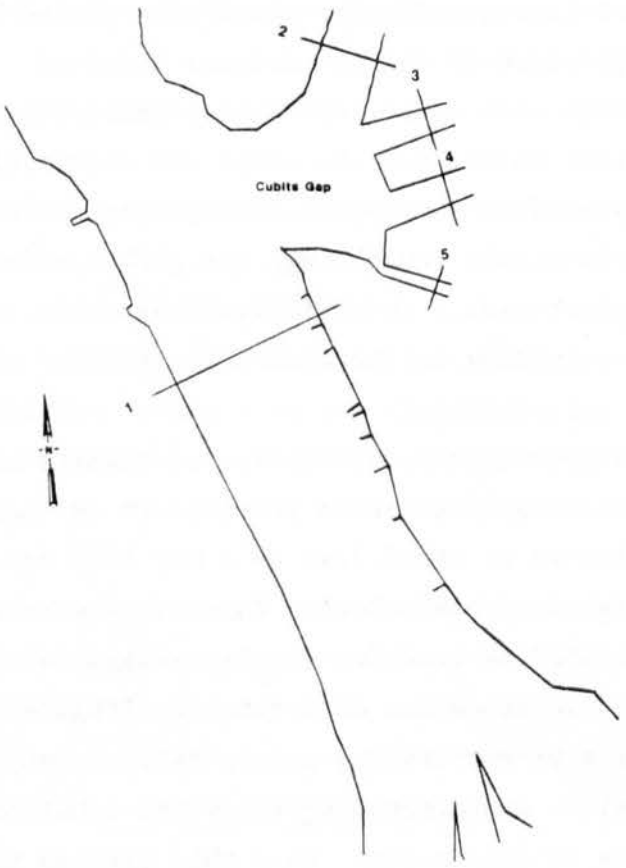

Figure 12. Location of velocity stations

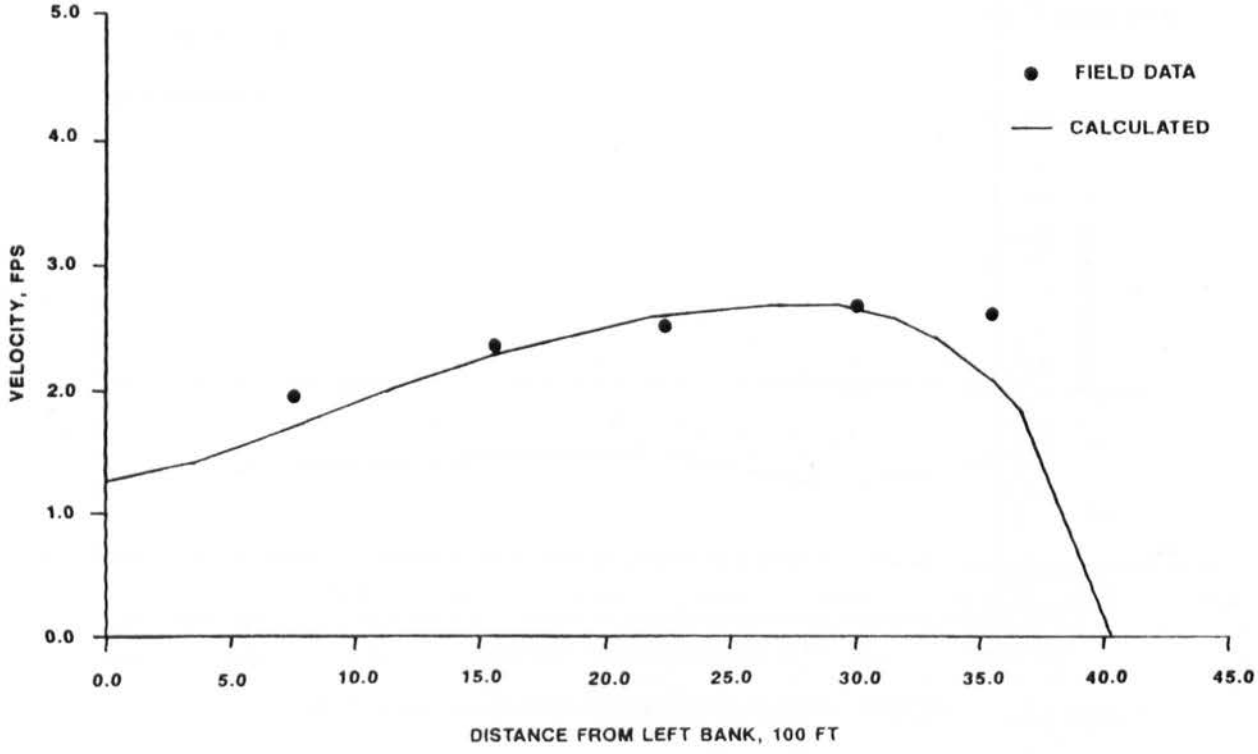

Figure 13. Velocity verification, sta 1

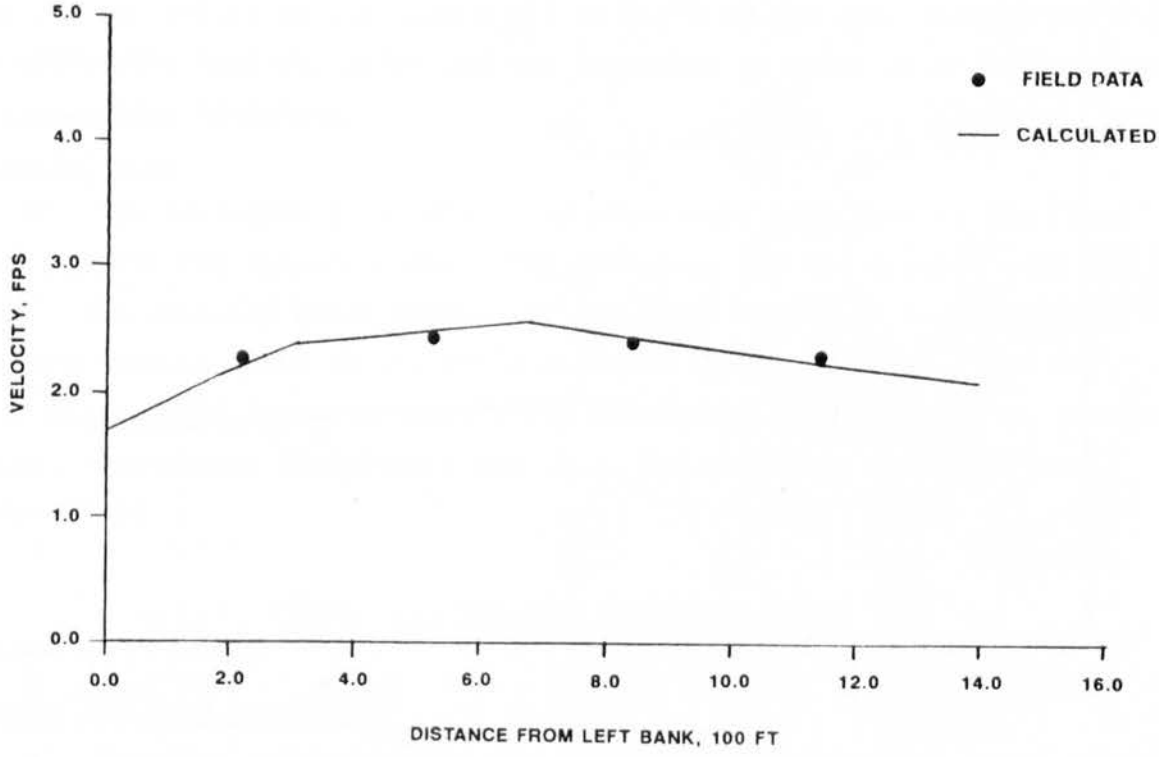

Figure 14. Velocity verification, sta 2

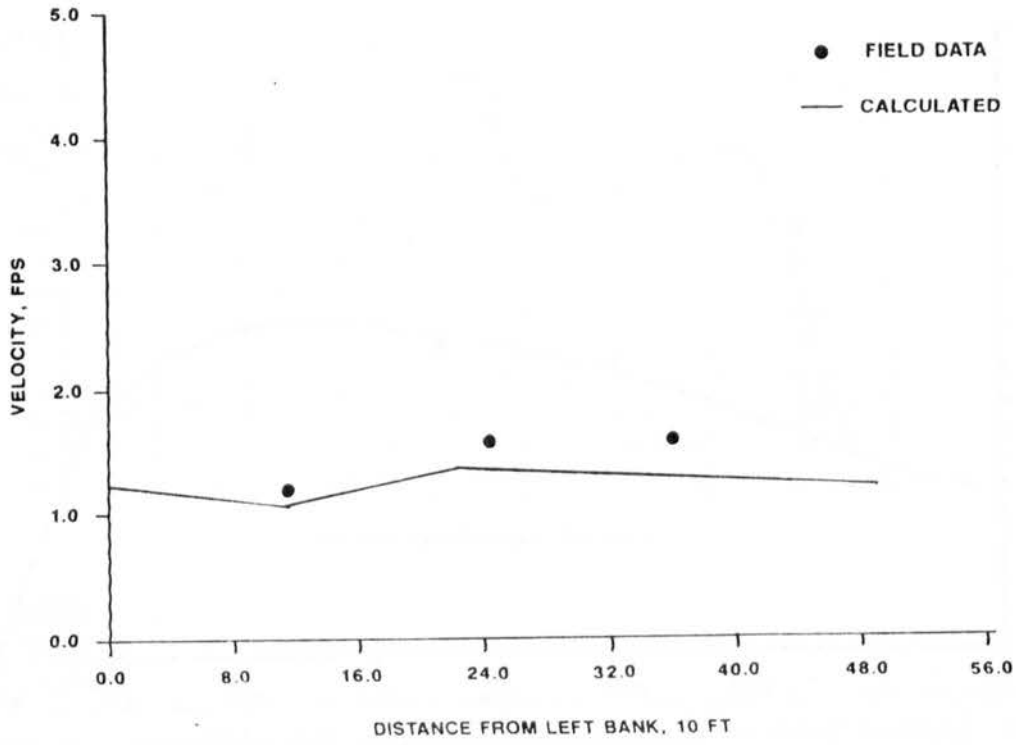

Figure 15. Velocity verification, sta 3

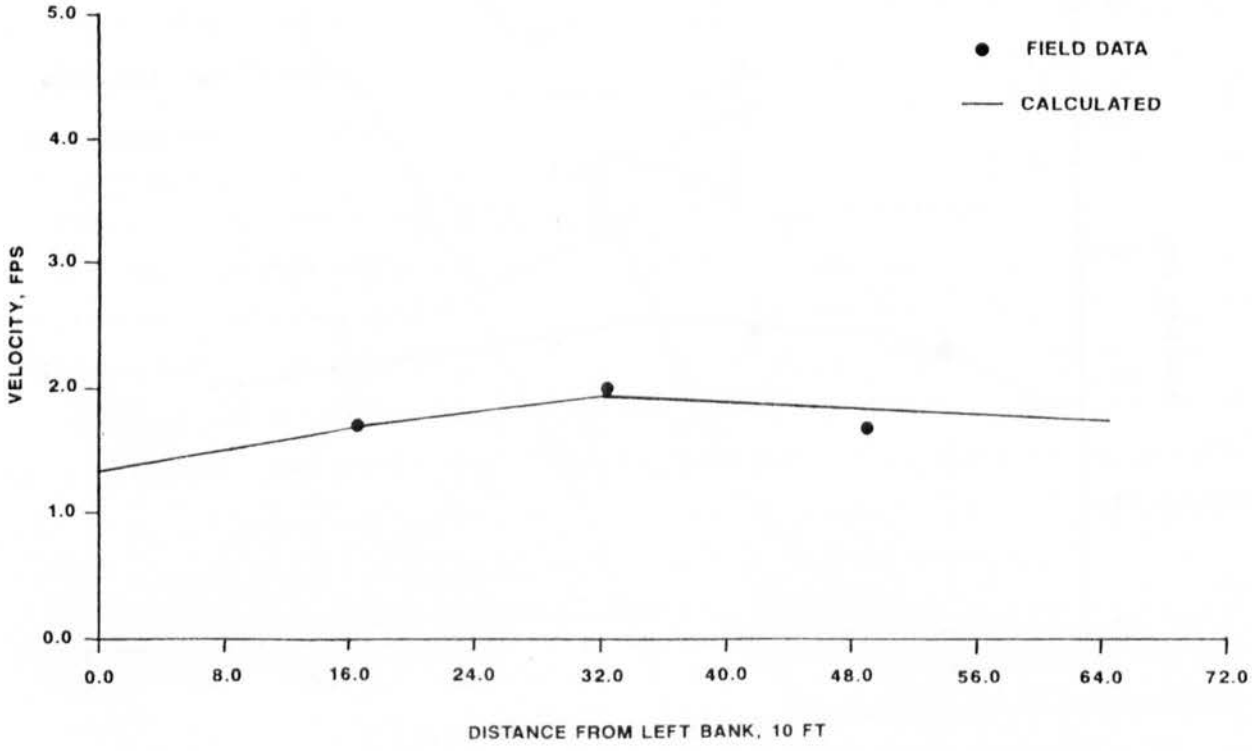

Figure 16. Velocity verification, sta 4

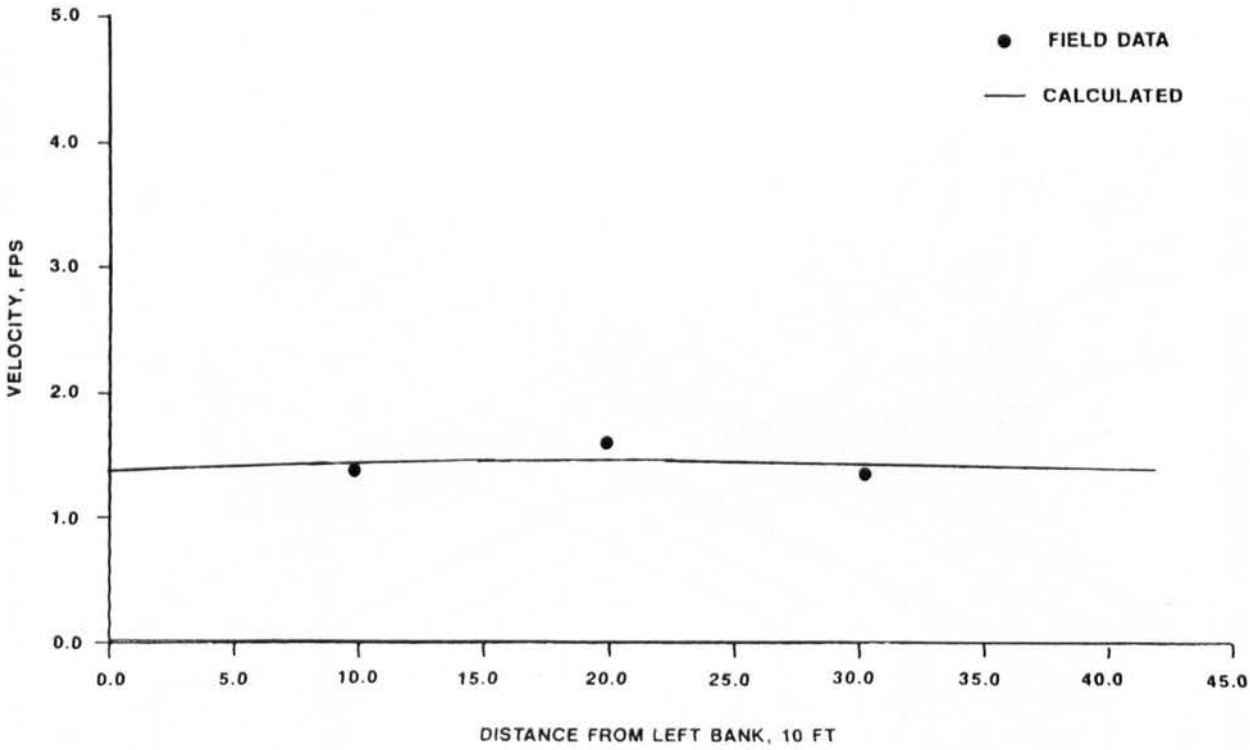

Figure 17. Velocity verification, sta 5

model was reproducing the flow conditions and distributions as measured on 2 May 1989. The final eddy viscosity coefficient was 100 lb-sec/ft^2. Manning's n values varied from 0.015 to 0.020 in the main channel and 0.025 to 0.067 in the distributaries and was dependent on water depth, vegetative cover, and flow conditions.

Hydrograph runs

19. The histogram flows discussed previously were used as the input hydrograph for the dynamic model. The time-step for the dynamic runs was 15 min. The computed nodal velocities and water depths at each time-step were saved and used as input to the STUDH sediment transport model. The velocity vector plots under high-flow conditions (discharge 1,120,000 cfs at Tarbert Landing, approximate Carrolton stage 17.0) for each case are shown in Figures 18-23.

Numerical Sediment Transport Model

Boundary and flow conditions

20. Boundary conditions for the STUDH sediment transport model consisted

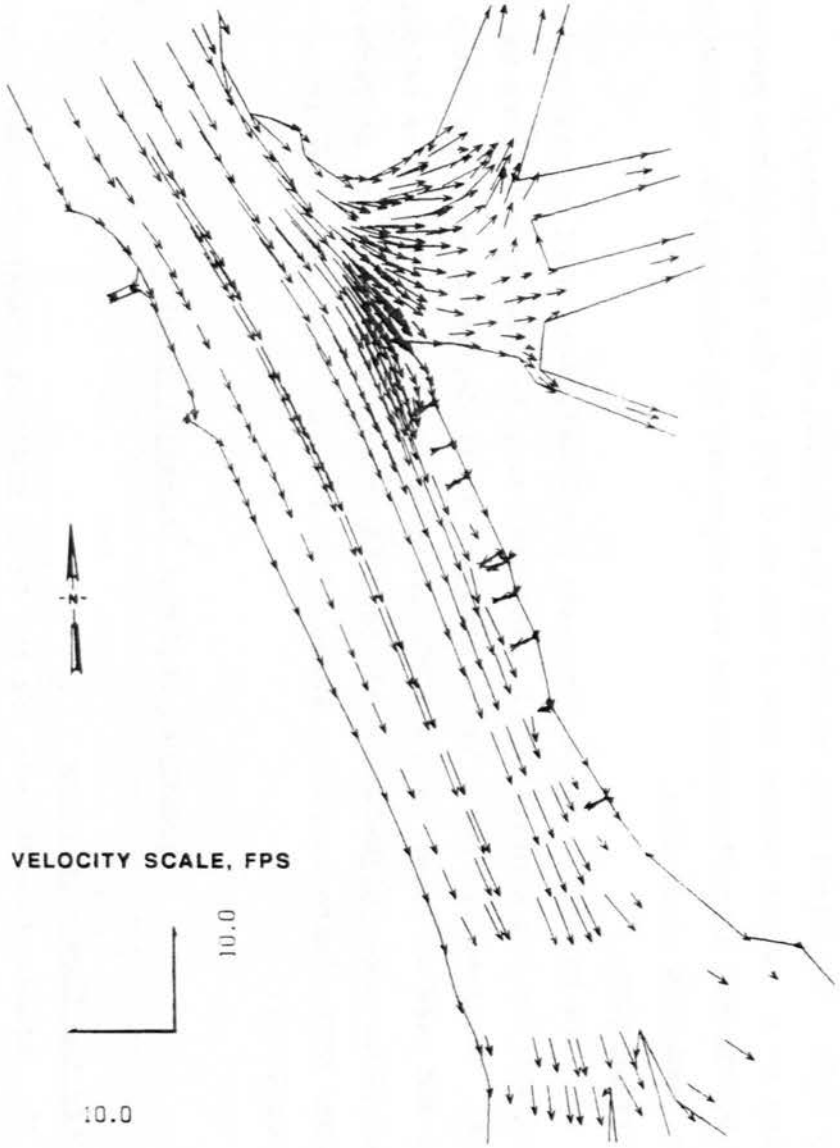

Figure 18. Velocity vectors, base condition

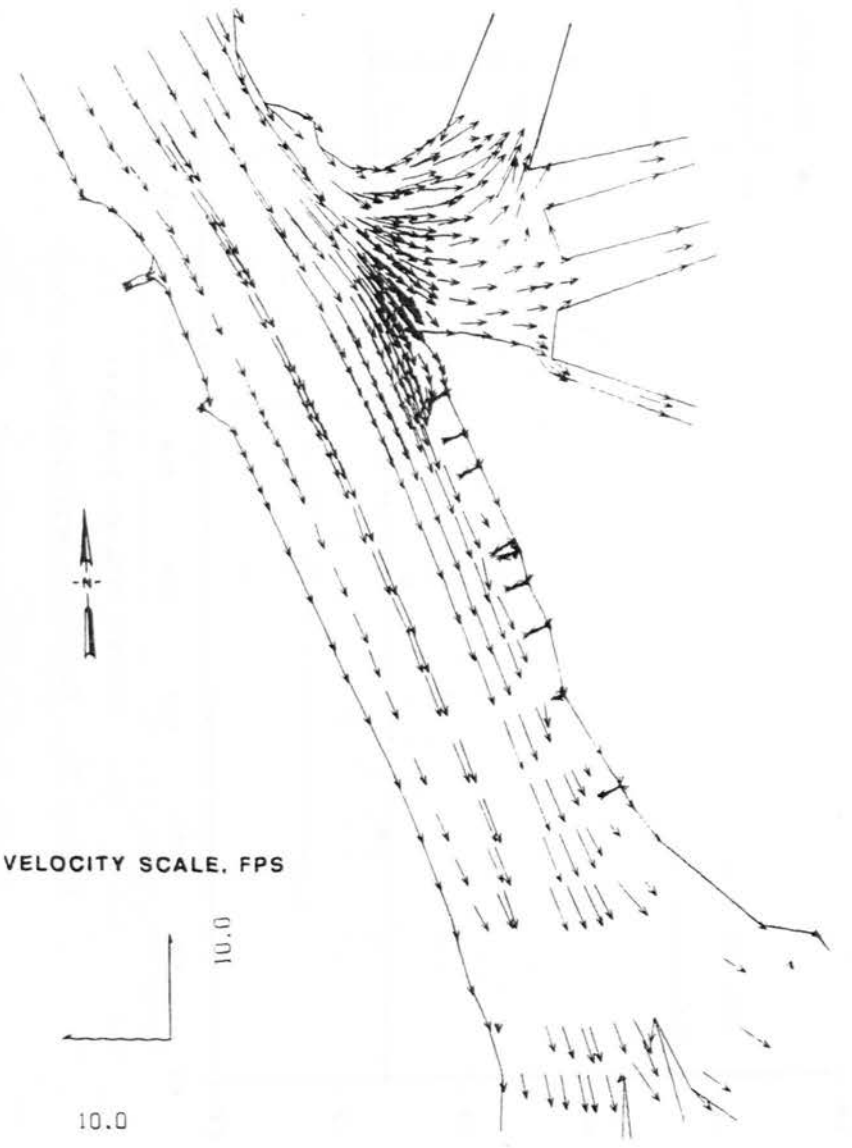

Figure 19. Velocity vectors, advance maintenance plan

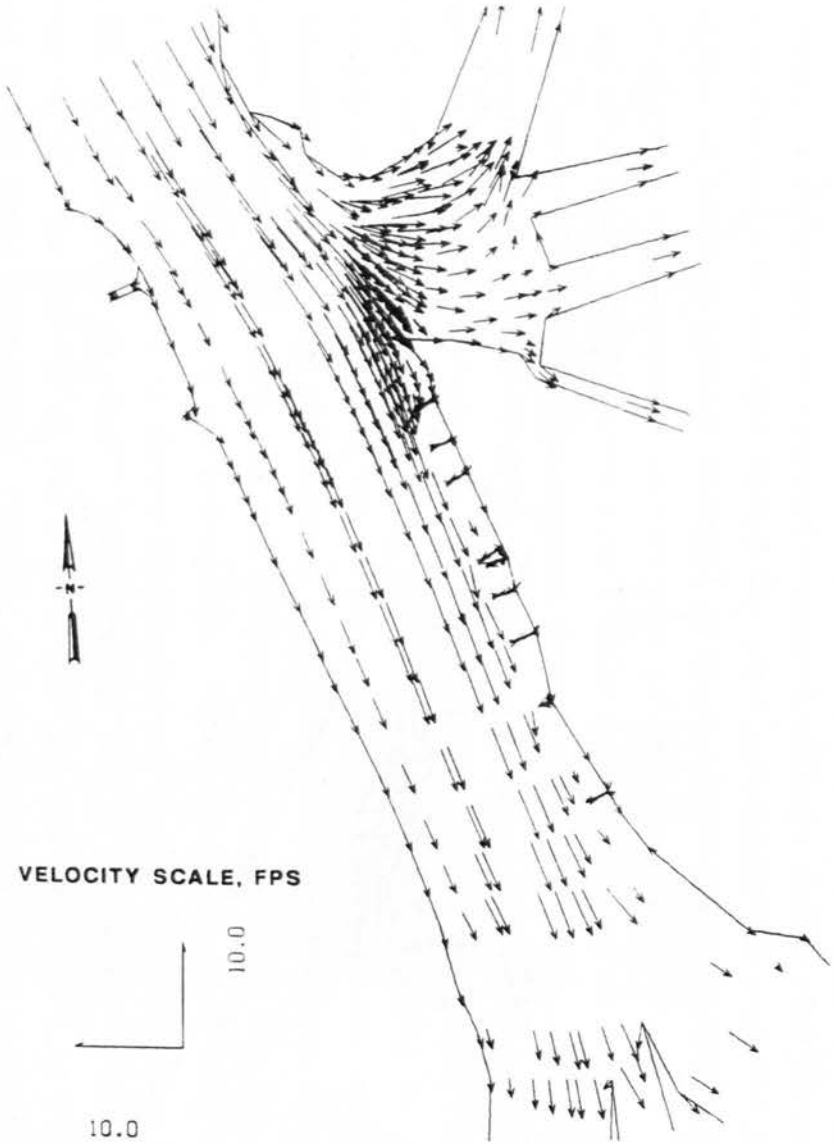

Figure 20. Velocity vectors, sediment trap plan

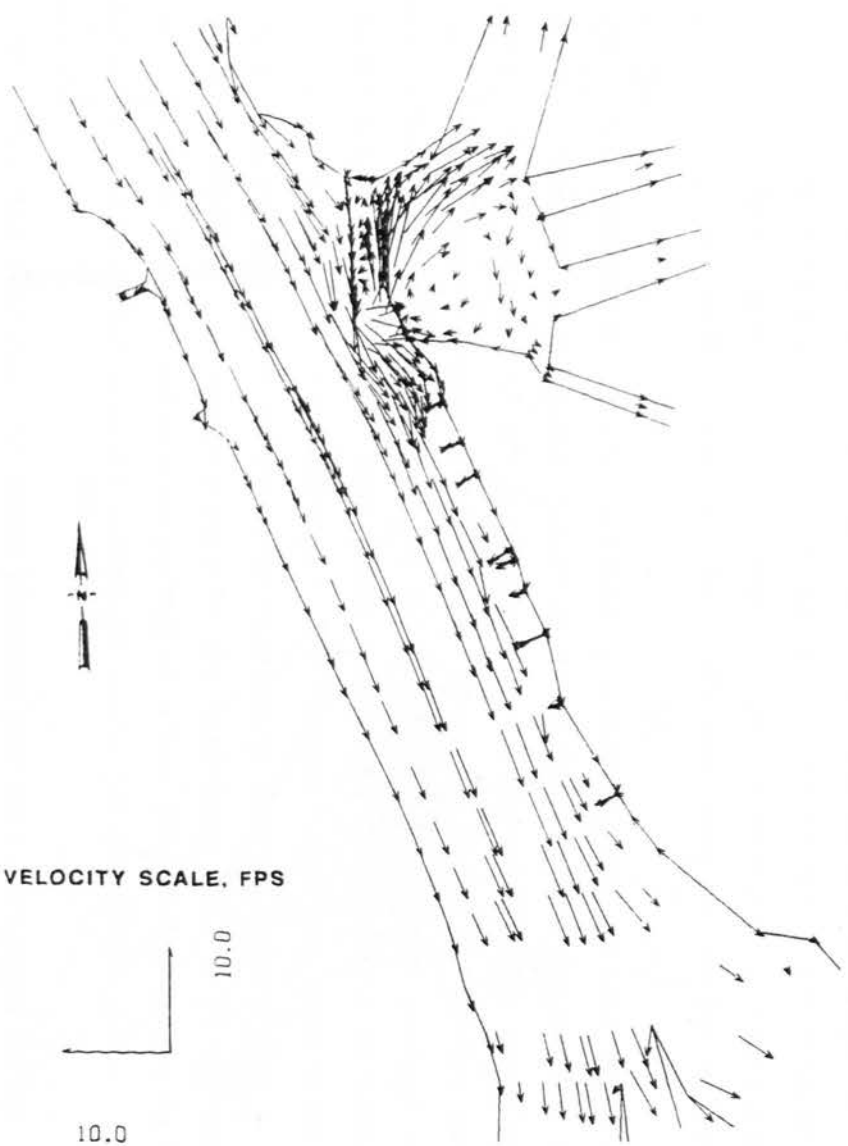

Figure 21. Velocity vectors, dike plan 1

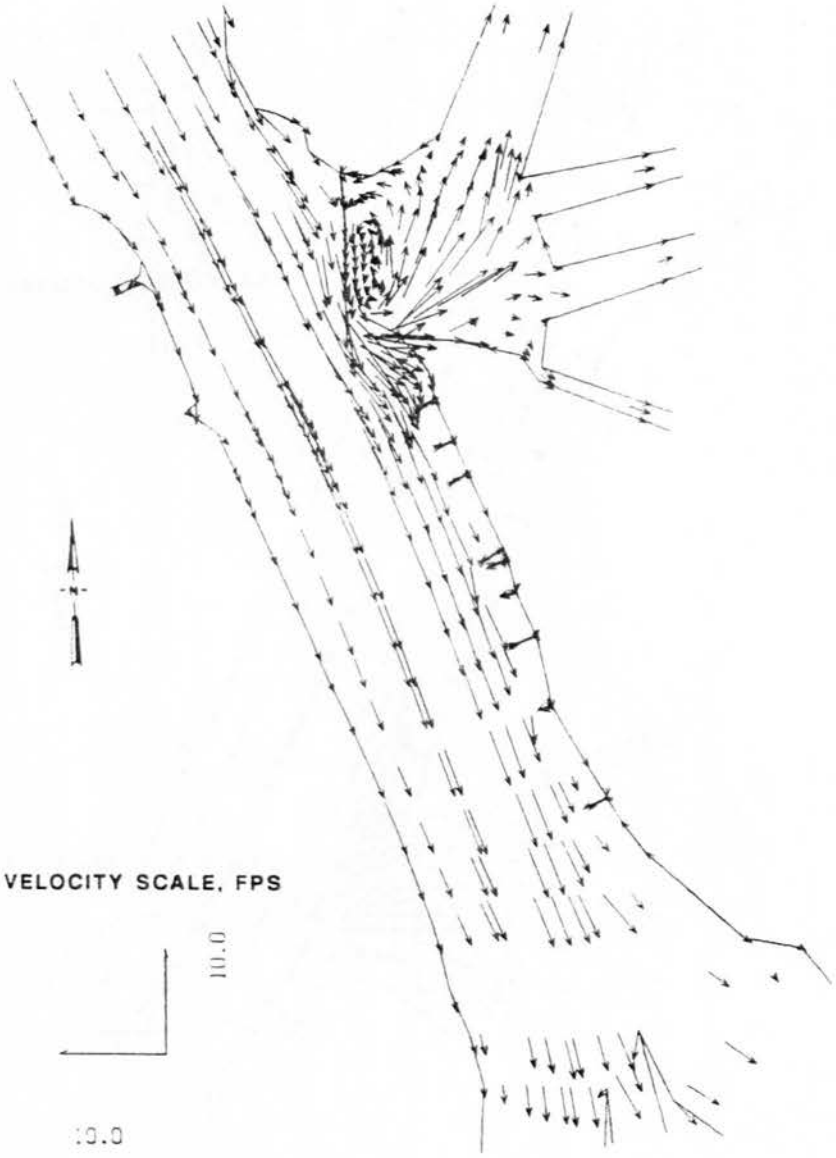

Figure 22. Velocity vectors, dike plan 2

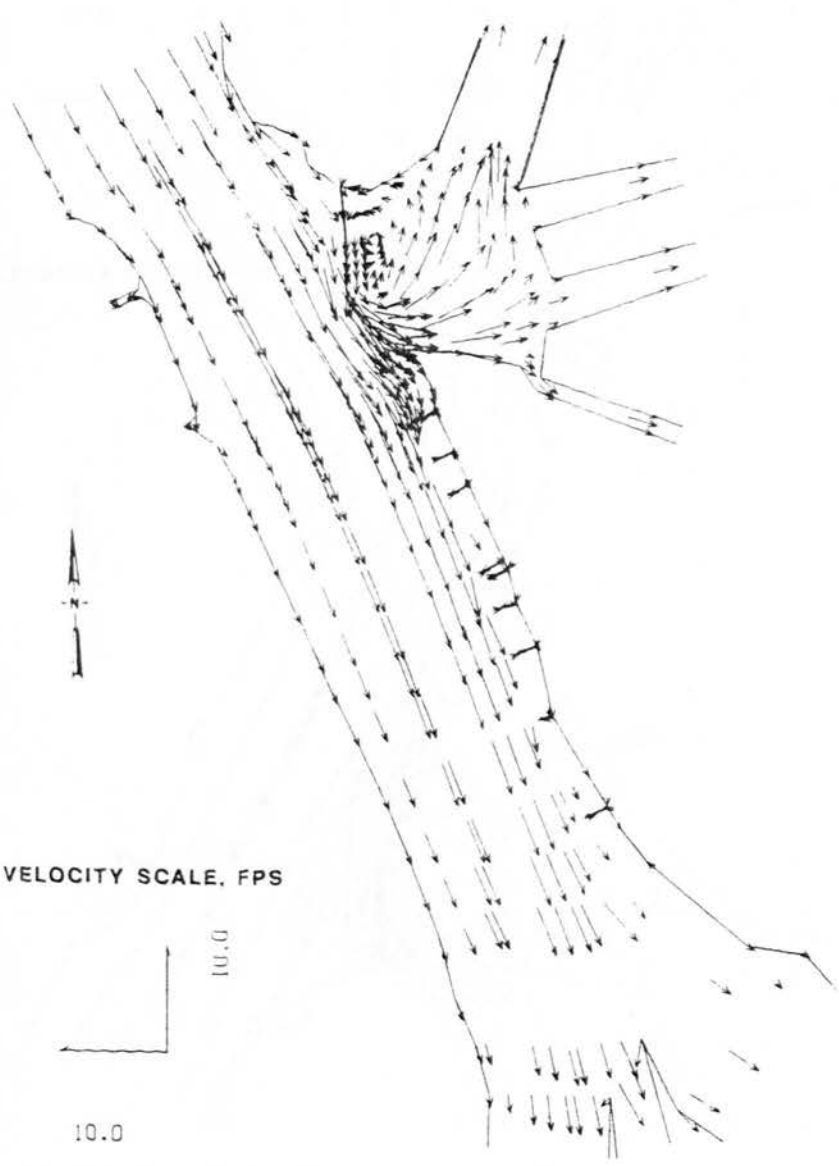

Figure 23. Velocity vectors, dike plan 3

of suspended sediment concentrations. The nodal velocities as computed by the hydrodynamic model were saved and used to update the velocity field in the model at the beginning of each time-step. Suspended sediment concentrations measured during the field survey on 2 May 1989 were used as initial values.

Verification

21. The sediment model was verified by adjusting the various input variables until the model reproduced actual shoaling volumes and the spatial distribution of the sediment in the study reach. This procedure was begun by making a large number of sensitivity runs. These consisted of a 7-day period (6 May-12 May 1989) of actual flows in which the variables were changed and the model responses recorded. This phase culminated when results on either side of an optimum value were obtained. The optimum value was that which produced shoaling and scour in patterns similar to those obtained from field hydrographic surveys that corresponded to the beginning and end of the test period. This battery of tests also served to allow later adjustments to be made rapidly and provided a solid technical basis for parameter value selection.

22. Once the shoaling and scour patterns had been initiated in the correct locations and at observed rates, the entire 87-day hydrograph histogram was input. A comparison of computed suspended sediment values with those input at the upstream boundary showed the input concentrations were too low. These were adjusted to reflect averages of those computed at interior nodes. A plot of these concentrations against time is shown in Figure 24.

23. The STUDH code uses the Ackers-White sediment transport function for computing noncohesive sediment transport (Ackers and White 1973). This is a single grain size function; that is, the entire sediment distribution is assumed to be characterized by the D_{35} size fraction. This assumption was not entirely satisfactory when attempting to reproduce rates of shoaling for both the rising and falling limbs of the inflow hydrograph with the same values. To compensate for this and to reproduce more accurately the observed values, a different Manning's n value for bed shear stress was specified for the rising and falling limbs of the hydrograph. This numerical method worked quite well and is founded in theory that indicates that the bed material is subject to sorting due to scour. Additionally, the n value also reflects, to some extent, the effects of bed forms, which are also different at various points in the flood hydrograph. Finally, the computational time-step was

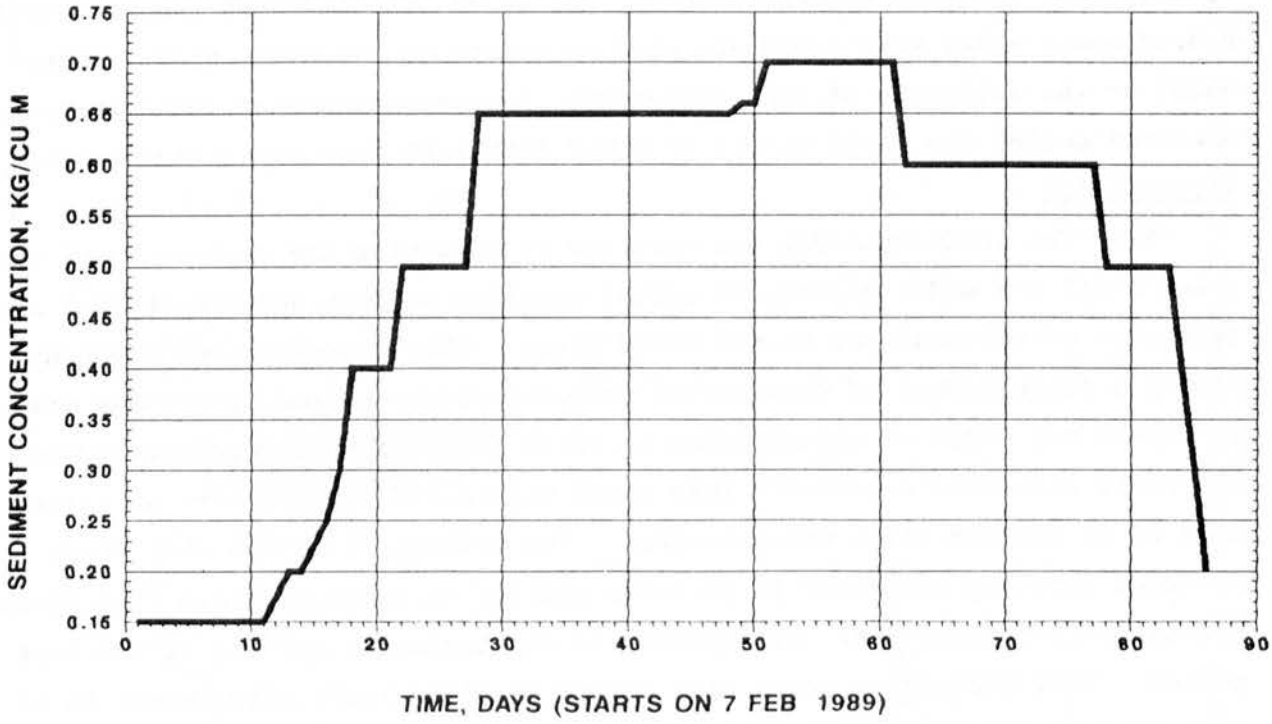

Figure 24. Verification sediment concentration used at boundary

fine-tuned and a duration of 15 min was selected. The final model parameter values are summarized in the following tabulation:

Parameter	Value
Crank-Nicholson implicitness factor	0.67
Manning's n for bed shear stress (rising limb)	0.03
Manning's n for bed shear stress (falling limb)	0.02
Effective particle diameter for transport, mm	0.15
Effective settling velocity, m/sec	0.014
Diffusion coefficient, m^2/sec	5

24. Based on dredging records obtained from the New Orleans District, 2,760,000 cu yd of material were dredged from the study reach, miles 0.0-4.0 AHP, during the period 7 February to 4 May 1989. The verified sediment model predicted 2,810,000 cu yd. This 2 percent variance was considered excellent for a volumetric check of the model's ability to reproduce prototype shoaling volumes.

25. Hydrographic surveys made periodically during the February-May period by the New Orleans District were used to check the model's ability to reproduce shoaling distribution. Prior to the end of March, the dredging

effort in the study reach was limited. After the end of March, dredging activities corrupted the accuracy of the surveys for determining shoaling heights. Therefore, comparisons were made of several pairs of surveys during the February-March timeframe to shoaling heights predicted by the model for the same periods. These comparisons demonstrated that the 2-D sediment model was predicting accurately the formation and location of individual shoals.

26. The results of the volumetric verification are summarized in Table 1. Table 2 contains the distribution verification summary. From these, it can be seen that the 2-D sediment model was quite accurately reproducing not only observed shoaling volumes, but also shoaling heights and locations within the navigation channel.

PART III: MODEL RESULTS

Hydrodynamics

27. The verified model was also used to check the percent of flow passing through Cubits Gap. A range of flows and the corresponding flow as a percent of the total flow at Venice, LA, are summarized in the following tabulation:

Venice, LA, Discharge, cfs	Cubits Gap Flow percent of Venice Flow
534,000	15
758,000	14
960,000	14
1,120,000	14

28. These percentages are higher than the historical percentage of about 6 percent and higher even than the 9-11 percent predicted when the Supplement II works were completed (US Army Engineer District, New Orleans, 1984). They do, however, match measurements made by both WES and the New Orleans District during the spring of 1989.

29. The verified RMA-2V model was then adjusted to the test base condition by deepening the channel to the ideal depth of 48 ft. This was done to provide consistency with the previously mentioned one-dimensional model results and more accurately model conditions that normally exist in the study reach. Velocity vector plots for this condition in the study reach are shown in Figure 18.

30. Hydrodynamic results for the advance maintenance and sediment trap plans indicated decreased channel velocities, as one might expect from increasing the channel area without a corresponding increase in discharge. The percent of Venice flow that exited through Cubits Gap for each plan was similar to that for the base plan. Velocity vector plots for these two plans are shown in Figures 19 and 20.

31. The hydrodynamic results for the three dike plans showed more variation. Flows were accelerated locally off the tip of the dike angled towards the channel. As was discussed earlier, the 90- and 45-deg dike plans were eliminated early in the study because they had little effect. The velocity

vector plots for dike plans 1-3 are shown in Figures 21-23, respectively. The dikes not only changed the flow distribution, but also locally accelerated the velocities in the channel off the dike tips. This had the effect of increasing the sediment transport capacity locally and reducing deposition at the previous locations near Cubits Gap. The effect of the dikes on the flow distribution at Cubits Gap for various flows is shown in the following tabulation. It can be seen that dike plan 1 returns the flow distribution at Cubits Gap to the amount expected with the Supplement II works in place.

Venice, LA, Discharge, cfs	Percent of Venice Flow Exiting Cubits Gap		
	Dike 1	Dike 2	Dike 3
534,000	11	14	14
758,000	9	12	13
960,000	9	12	12
1,120,000	8	12	12

Sedimentation

32. The total shoaling, average shoaling per day, and maximum shoaling per day for the base condition and each plan are shown in Table 1. These do not fully form a basis for comparison of the results of the various plans. Therefore, an index was computed for each condition. This number is derived by dividing the maximum daily shoaling by the average daily shoaling. The index is a measure of the maximum shock to the system due to shoaling and is termed the shock shoaling index. It indicates the likelihood that on-site dredging plant will be unable to keep up with the peak shoaling rates. The indexes for the various conditions are summarized in the following tabulation:

Condition	Shock Shoaling Index
Base	3.49
Advance maintenance	3.38
Sediment trap	3.59
Dike 1	2.27
Dike 2	3.09
Dike 3	3.41

An index of 1.00 would indicate that the average dredging capacity could also keep up with the maximum shoaling rate. The higher this number, the greater

the risk of losing the authorized navigation channel depth due to a shock loading of sediment. The indexes are an abstract measure of the reaction time available to add additional dredge plant to the site to maintain the authorized project dimensions.

33. For each condition, color plots were generated to indicate graphically areas of scour and shoaling. Other color plots show the suspended sediment concentration distribution. These plots were derived based on the spring 1989 hydrograph, 7 February-4 May. For convenience and comparison, the hydrograph was broken at 28 March. This allowed the two peaks of the hydrograph to be observed separately. Additionally, when the second hydrograph was begun, the channel was returned to the initial bottom elevation. This allowed more realistic shoaling rates to be computed and reflected the fact that real-time dredging removed a large portion of the shoaled material in the prototype.

34. The performance of the plans was also evaluated based on total channel area affected by loss of navigation depth. For this evaluation, the model was run with no allowance for dredging of deposited material. The first 50 days of the spring 1989 hydrograph were used for this comparison. The areas where navigation depth was lost for each condition are shown in Figures 25-30. These results are quantified in the following tabulation:

Condition	Shoaling Above El -45, acres*
Base	229
Advance maintenance	195
Sediment trap	315
Dike 1	68
Dike 2	78
Dike 3	105

* Total channel area 320 acres.

35. Table 1 and Figures 26 and 27 indicated that the sediment trap plan provided no advantage over the advance maintenance plan in maintaining project depths. In fact, the sediment trap plan exacerbated the problem of maintaining project depth in the navigation channel by increasing both the amount of dredging and its areal extent. Ships moored in the deepened sediment trap would set up perturbations in the flow field that could affect navigation

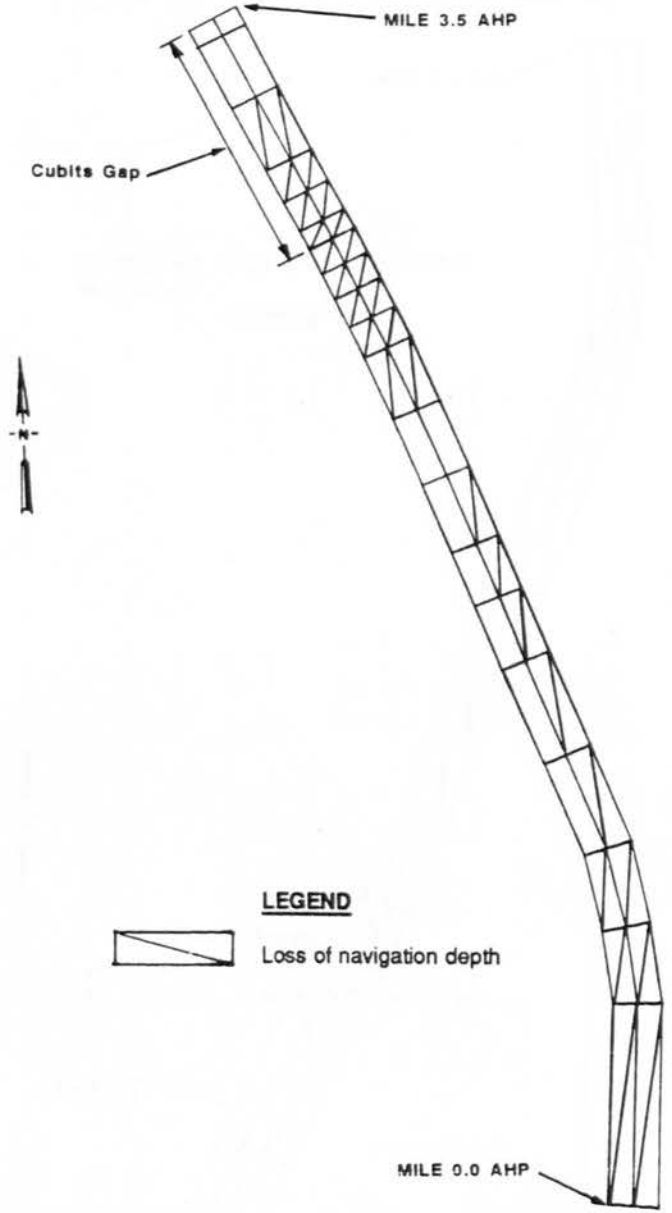

Figure 25. Base condition, loss of navigation depth

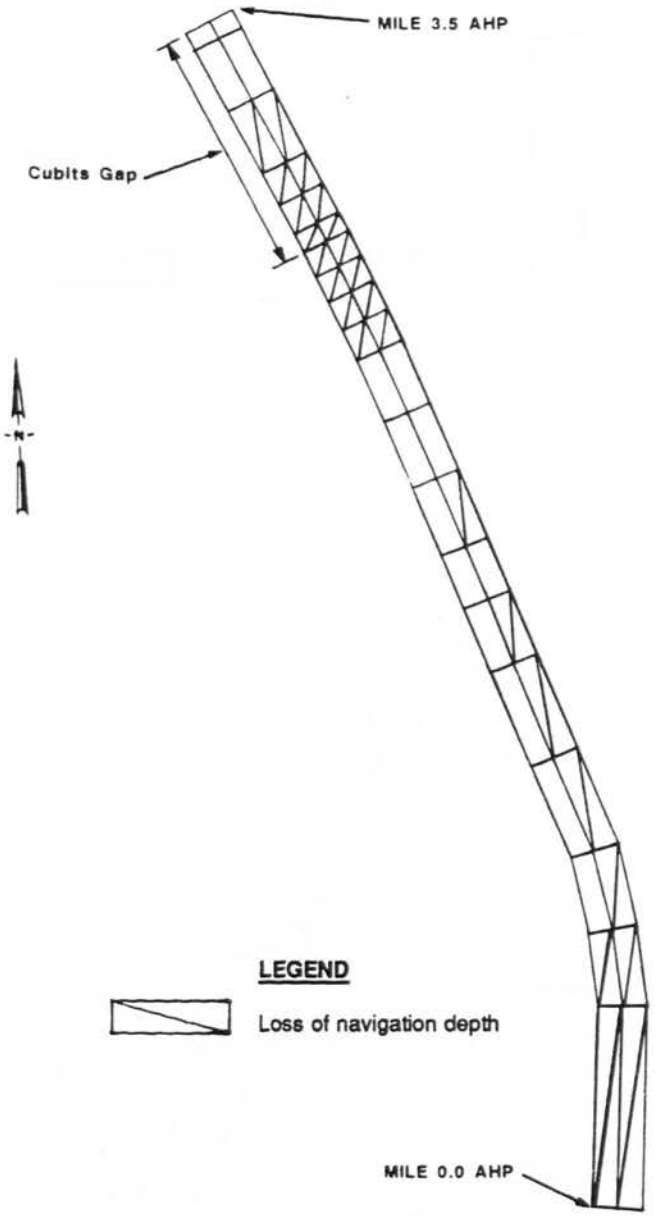

Figure 26. Advance maintenance, loss of navigation depth

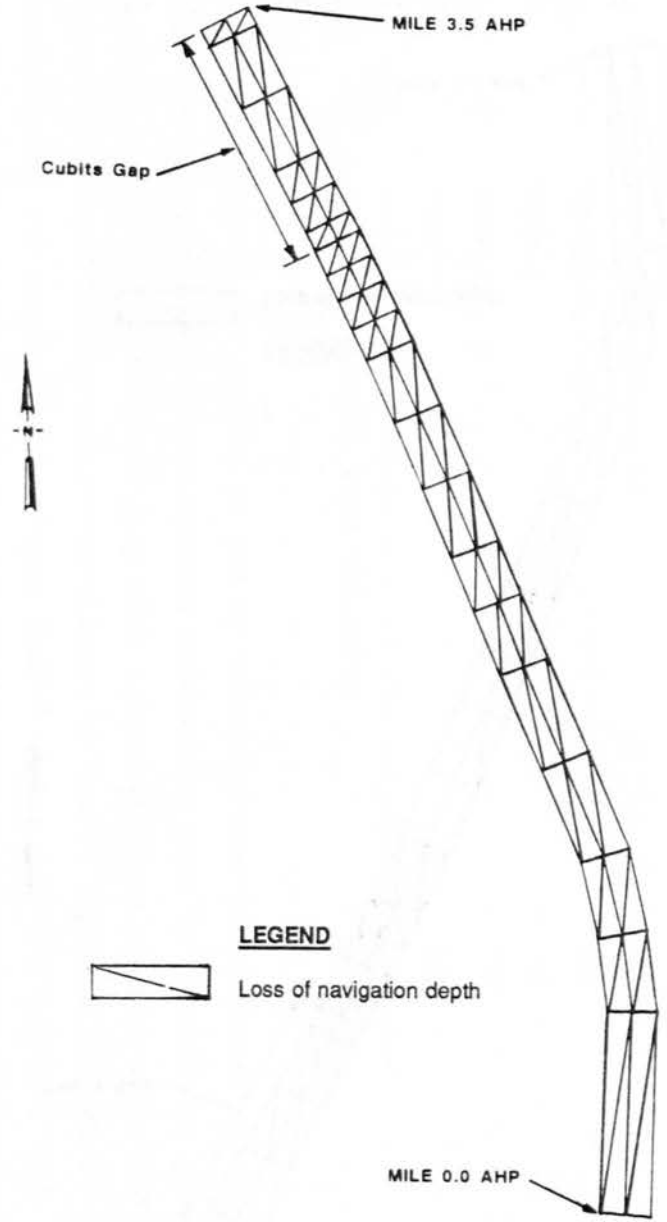

Figure 27. Sediment trap, loss of navigation depth

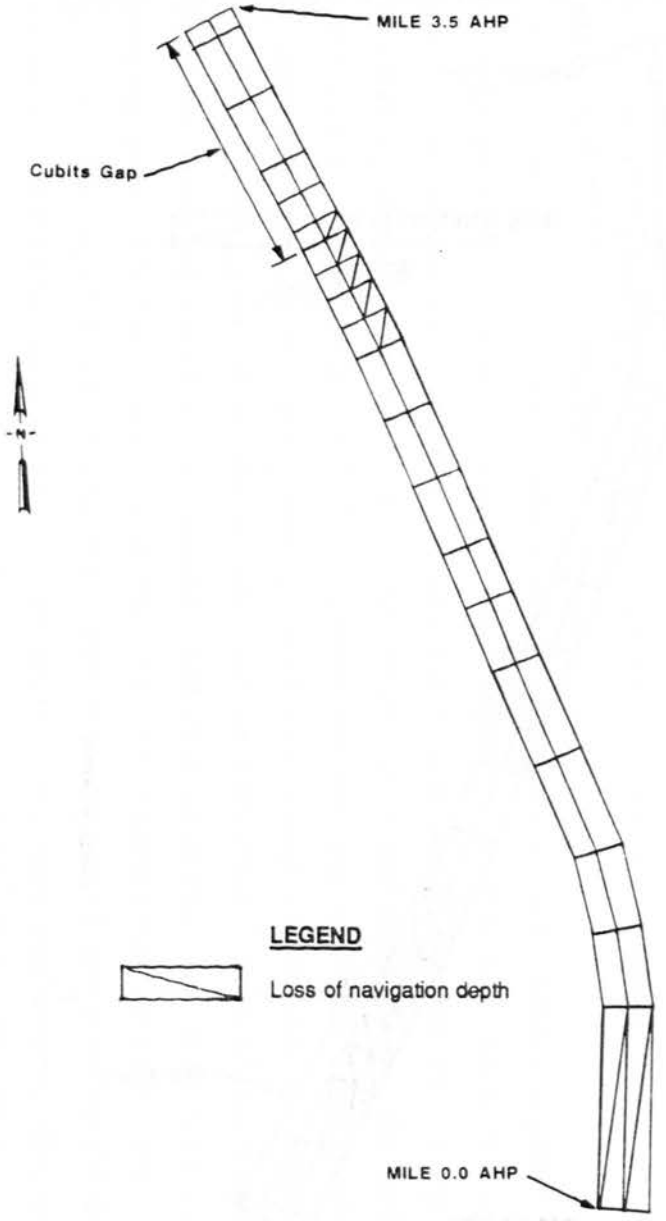

Figure 28. Dike plan 1, loss of navigation depth

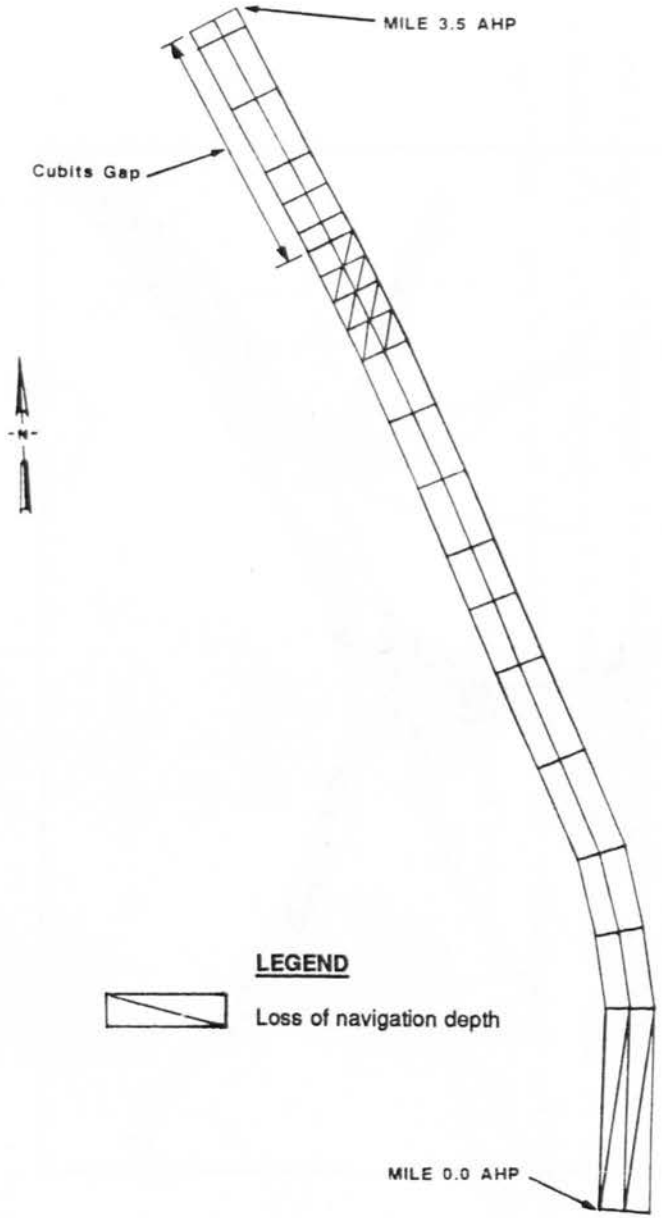

Figure 29. Dike plan 2, loss of navigation depth

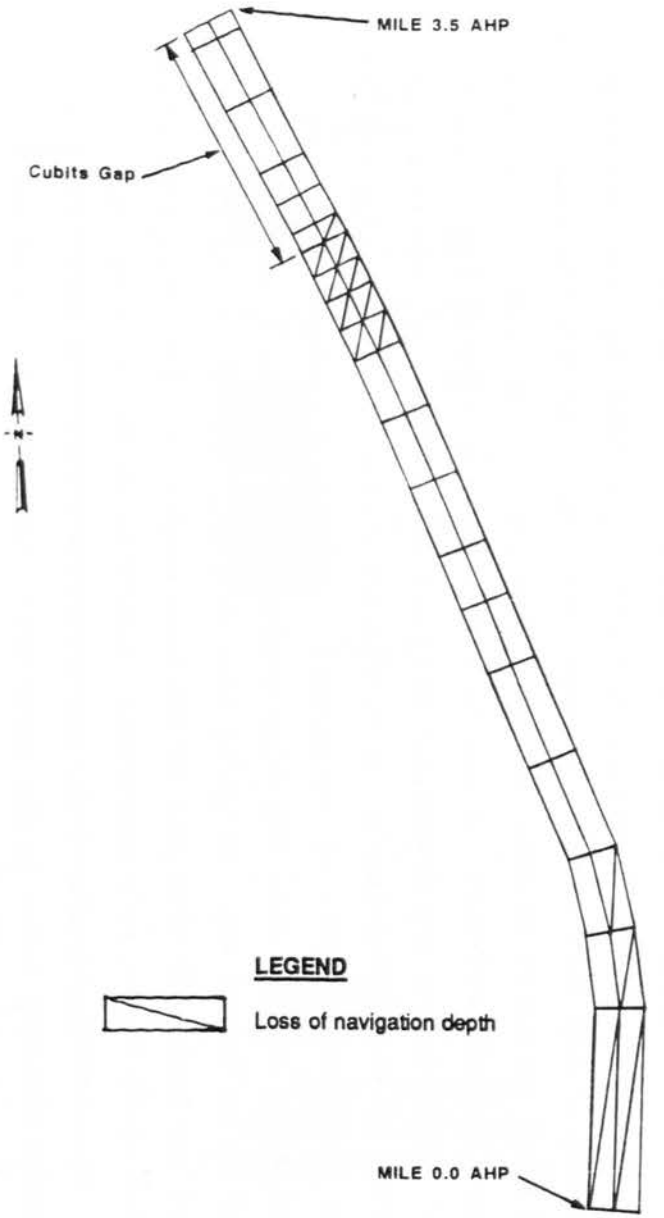

Figure 30. Dike plan 3, loss of navigation depth

safety and increase shoaling in the channel. It should be noted that both nonstructural plans would require more dredging than the base condition.

36. Table 1 also indicated that plan 1 provided the least amount of shoaling of any plan tested. Figures 26-30 indicated that the shoaling that did occur tended to be more localized than that in the nonstructural plans. Figure 21 indicated that the upstream angle dike created a flow separation that reattached on the downstream headland dike. This resulted in a higher percent of flow remaining in the navigation channel and increasing the sediment transport capacity of the channel. Additionally, flows were locally accelerated off the dike tip which tended to prevent the formation of the shoal below Cubits Gap. Slightly more shoaling occurred at the HP, but the total was much less than that of the base condition. All three dike plans tested would result in a substantial reduction in channel shoaling.

37. At the request of the New Orleans District, the model was used to forecast shoaling rates in the study area. One forecast period was 24 January-25 February 1990 and the other was 3 March-26 March 1990. The model predictions of volume and area of shoaling appeared reasonable. Advance maintenance dredging during the prediction period prevented field verification of the shoaling predictions. However, the technique developed demonstrated that the previously verified 2-D sediment model could be used to produce predictions rapidly for periods of up to 30 days.

38. Figure 31 is a black and white example of a typical scour and deposition color plot described in paragraph 33. Appendix B provides a complete set of color plots of model-predicted bed change and suspended sediment concentration distribution for each condition at the end of the 7 February-28 March 1989 and 29 March-4 May 1989 hydrograph.

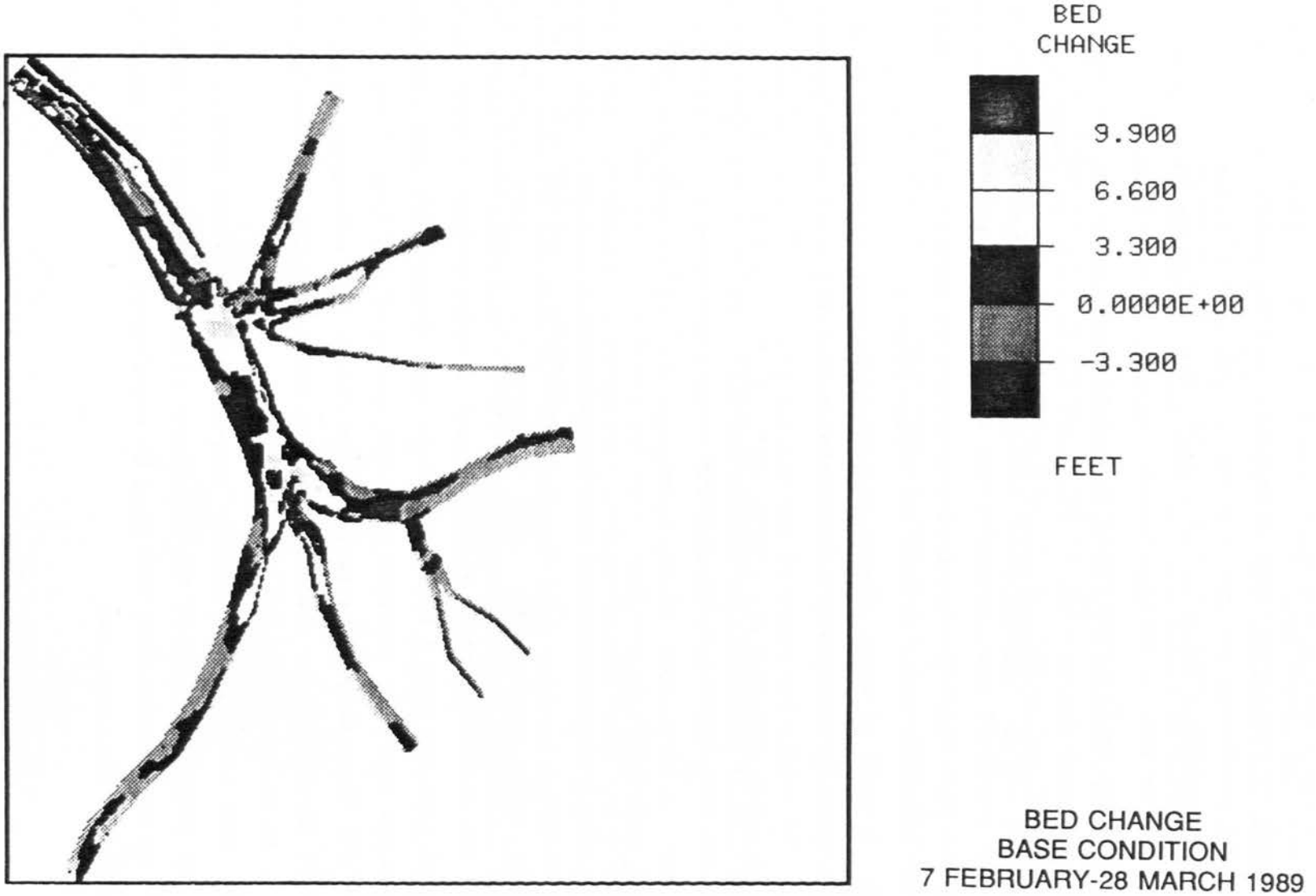

Figure 31. Example of scour and deposition plot. Appendix B presents a complete set of bed change and suspended sediment concentration distributions in color

PART IV: CONCLUSIONS

39. A two-dimensional model of the Mississippi River at Cubits Gap was constructed and verified to reproduce total dredging quantities and locations of shoaling accurately for the existing bathymetry and chosen input hydrograph. The developed model could be useful for estimating shoaling response to a variety of medium- to high-flow hydrographs in nearly real-time (i.e., shoaling could be predicted in daily increments in response to predicted hydrograph fluctuations). The model can be used for future analyses involving alternative channel geometries or combinations of structures with minor mesh modifications. While its use was for screening rather than design purposes, a more refined version of the model with more rigorous boundary condition treatment could be used for design purposes.

40. A total of seven channel modifications were tested and five of these were evaluated for their ability to minimize shoaling and loss of project depth in the Cubits Gap reach of the Mississippi River. They included the nonstructural alternatives of advance maintenance and a longitudinal sediment trap on the west side of the navigation channel and three structural plans at Cubits Gap. A large-flow, 87-day hydrograph was used to determine the performance of each plan.

41. The best nonstructural plan was advance maintenance. It provided a smaller shoaling quantity than the sediment trap plan and affected a smaller area of the navigation channel. Both nonstructural plans, however, would increase the channel shoaling rate compared to existing conditions. The best structural plan was plan 1 with a 2,800-ft-long 30-deg angle dike and 800-ft-long headland dike. It provided the least amount of shoaling of any plan tested. All three dike plans tested would result in a substantial reduction in channel shoaling. The shoaling that did occur tended to be more localized than that in the nonstructural plans.

42. This study did not address long-term sedimentation effects within Cubits Gap proper. If one of the structural plans is selected for implementation, it is recommended that this plan be reevaluated in depth to optimize the performance of the structure.

REFERENCES

Ackers, P., and White, W. R. 1973 (Nov). "Sediment Transport: New Approach and Analysis," Journal, Hydraulics Division, American Society of Civil Engineers, Vol 99, No. HY11, pp 2041-2060.

Ariathurai, R., MacArthur, R. C., and Krone, R. B. 1977 (Oct). "Mathematical Model of Estuarial Sediment Transport," Technical Report D-77-12, US Army Engineer Waterways Experiment Station, Vicksburg, MS.

Bragg, Marion. 1977. Historic Names and Places on the Lower Mississippi River, Mississippi River Commission, Vicksburg, MS.

Copeland, Ronald R. "Dredging Alternatives Study, Cubits Gap, Lower Mississippi River; TABS-1 Numerical Model Investigation" (in preparation), Report 1, US Army Engineer Waterways Experiment Station, Vicksburg, MS.

Fagerburg, T. L., "Mississippi River at Cubits Gap and Grand Pass; Field Data Report" (in preparation), US Army Engineer Waterways Experiment Station, Vicksburg, MS.

Norton, W. R., King, I. P., and Orlob, G. T. 1973. "A Finite Element Model for Lower Granite Reservoir," prepared for US Army Engineer District, Walla Walla, Walla Walla, WA.

Richards, D. R., and Trawle, M. J. 1987 (Jun). "A Numerical Model Analysis of Mississippi River Passes Navigation Channel Improvements; 55-Foot Channel Tests," Report 1, Miscellaneous Paper HL-87-2, US Army Engineer Waterways Experiment Station, Vicksburg, MS.

_____. 1988 (Sep). "A Numerical Model Analysis of Mississippi River Passes Navigation Channel Improvements; 45-Foot Channel Tests and Flow Diversion Schemes," Report 2, Miscellaneous Paper HL-87-2, US Army Engineer Waterways Experiment Station, Vicksburg, MS.

US Army Engineer District, New Orleans. 1984. "Mississippi River, Baton Rouge to the Gulf, Louisiana," Draft Environmental Impact Statement, Supplement II, Appendix E, New Orleans, LA.

Table 1

Volumetric Verification and Results of the 2-D Sediment Model

7 February-4 May 1989, Miles 0.0-4.0 Above Head of Passes

Condition	Volume of Deposition cubic yards
Verification	
Actual dredged volume (prototype)	2,760,000
Existing, 45-ft channel (model)	2,810,000

Results

	Shoaling, cu yd/day		Total Shoaling cu yd
	Average	Maximum	
Existing, 48-ft channel (base test conditions)	39,000	136,000	3,370,000
Advance maintenance, 50-ft channel	45,000	152,000	3,880,000
Sediment trap, 50 ft deep	49,000	176,000	4,280,000
Dike plan 1	15,000	34,000	1,350,000
Dike plan 2	22,000	68,000	1,950,000
Dike plan 3	27,000	92,000	2,310,000

Table 2

Verification of the 2-D Sediment Model Shoaling Distribution

	Bed Change, ft			
	7 Feb-23 Mar 1989		7 Feb-27 Mar 1989	
Element	Model	Prototype	Model	Prototype
534	7.7	5.6	8.7	7.2
535	7.0	3.5	7.8	6.9
523	3.7	5.2	4.3	7.1
524	4.0	3.8	4.6	4.0
512	2.4	4.6	3.0	5.5
513	3.5	3.3	4.3	4.4
503	1.6	4.1	2.1	4.5
504	3.4	2.3	4.3	2.2
495	3.6	2.7	4.5	3.0
494	1.9	4.2	2.3	6.3
486	3.2	2.3	3.9	2.8
485	2.0	4.4	2.3	2.2
475	2.7	3.5	3.2	2.6
474	1.6	4.8	1.8	--
41	3.6	2.5	3.7	2.8
40	2.6	--	2.5	3.0
464	3.6	2.3	3.7	4.0
463	3.4	--	3.3	3.0
455	3.4	4.8	3.4	2.8
454	3.6	4.2	3.5	4.7
446	5.1	--	5.0	--
445	4.8	--	4.6	4.0
437	7.1	--	7.0	--
436	6.3	--	6.1	--
402	4.4	--	4.2	--
401	3.5	--	3.3	--
388	4.1	--	3.9	--
387	3.4	--	3.2	--
357	5.7	5.0	5.5	--
356	5.3	--	5.0	--

Note: -- indicates record corrupted by dredging.

APPENDIX A: THE TABS-2 SYSTEM

1. TABS-2 is a collection of generalized computer programs and utility codes integrated into a numerical modeling system for studying two-dimensional hydrodynamics, sedimentation, and transport problems in rivers, reservoirs, bays, and estuaries. A schematic representation of the system is shown in Figure A1. It can be used either as a stand-alone solution technique or as a step in the hybrid modeling approach. The basic concept is to calculate water-surface elevations, current patterns, sediment erosion, transport and deposition, the resulting bed surface elevations, and the feedback to hydraulics. Existing and proposed geometry can be analyzed to determine the impact on sedimentation of project designs and to determine the impact of project designs on salinity and on the stream system. The system is described in detail by Thomas and McAnally (1985).

2. The three basic components of the system are as follows:

   a. "A Two-Dimensional Model for Free Surface Flows," RMA-2V.

   b. "Sediment Transport in Unsteady 2-Dimensional Flows, Horizontal Plane," STUDH.

   c. "Two-Dimensional Finite Element Program for Water Quality," RMA-4.

3. RMA-2V is a finite element solution of the Reynolds form of the Navier-Stokes equations for turbulent flows. Friction is calculated with Manning's equation and eddy viscosity coefficients are used to define the turbulent losses. A velocity form of the basic equation is used with side boundaries treated as either slip or static. The model automatically recognizes dry elements and corrects the mesh accordingly. Boundary conditions may be water-surface elevations, velocities, or discharges and may occur inside the mesh as well as along the edges.

4. The sedimentation model, STUDH, solves the convection-diffusion

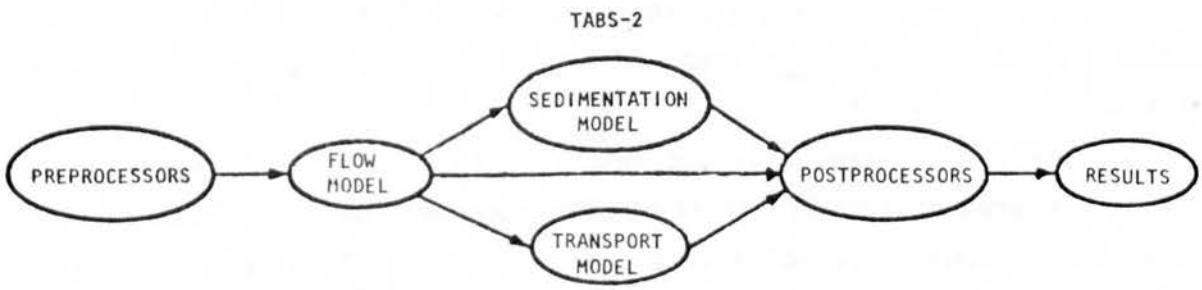

Figure A1. TABS-2 schematic

equation with bed source terms. These terms are structured for either sand or cohesive sediments. The Ackers-White (1973) procedure is used to calculate a sediment transport potential for the sands from which the actual transport is calculated based on availability. Clay erosion is based on work by Partheniades (1962) and Ariathurai and the deposition of clay utilizes Krone's equations (Ariathurai, MacArthur, and Krone 1977). Deposited material forms layers, as shown in Figure A2, and bookkeeping allows up to 10 layers at each node for maintaining separate material types, deposit thickness, and age. The code uses the same mesh as RMA-2V.

5. Salinity calculations, RMA-4, are made with a form of the convective-diffusion equation which has general source-sink terms. Up to seven conservative substances or substances requiring a decay term can be routed. The code uses the same mesh as RMA-2V.

6. Each of these generalized computer codes can be used as a stand-alone program, but to facilitate the preparation of input data and to aid in analyzing results, a family of utility programs was developed for the following purposes:

a. Digitizing
b. Mesh generation
c. Spatial data management
d. Graphical output
e. Output analysis
f. File management
g. Interfaces
h. Job control language

Finite Element Modeling

7. The TABS-2 numerical models used in this effort employ the finite element method to solve the governing equations. To help those who are unfamiliar with the method to better understand this report, a brief description of the method is given here.

8. The finite element method approximates a solution to equations by dividing the area of interest into smaller subareas, which are called elements. The dependent variables (e.g., water-surface elevations and sediment concentrations) are approximated over each element by continuous functions

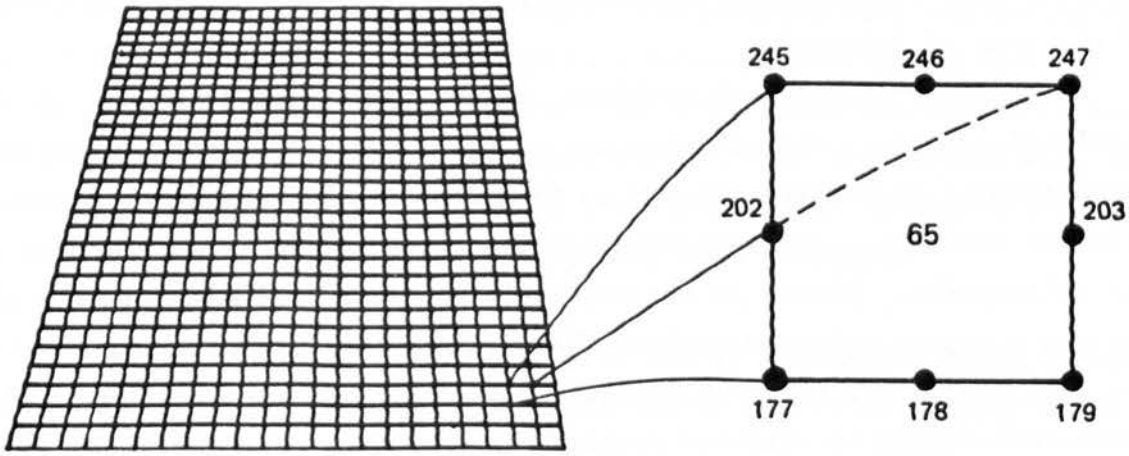

a. Eight nodes define each element

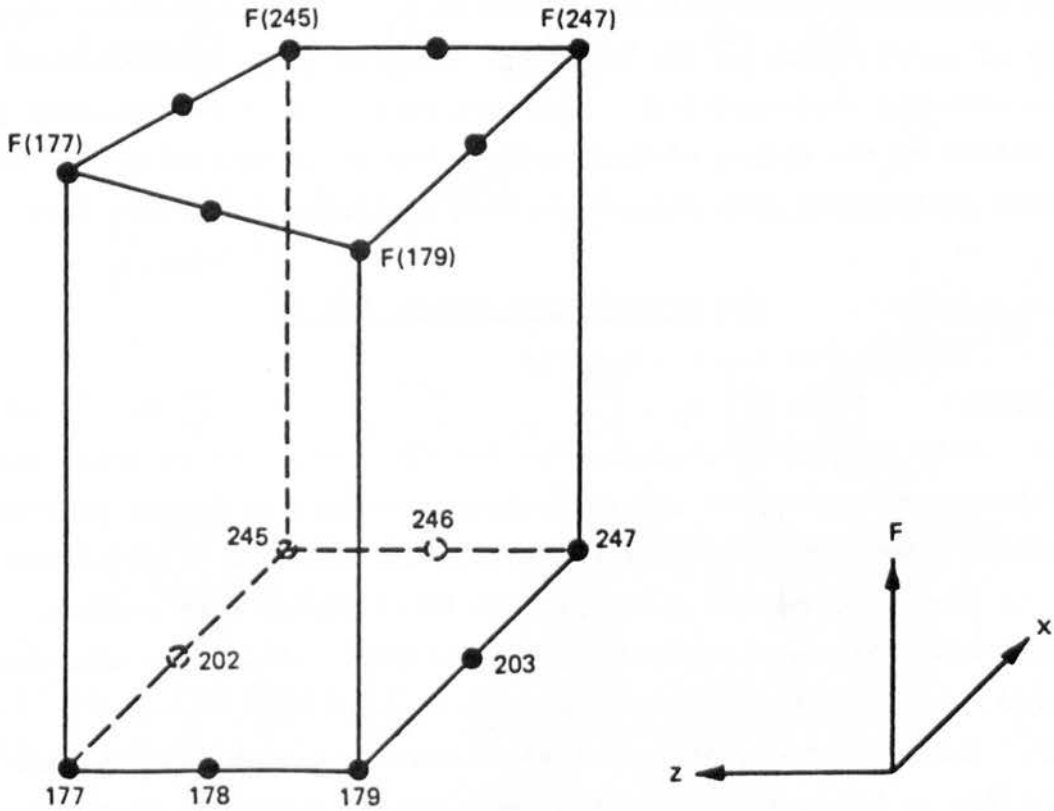

b. Linear interpolation function

Figure A2. Two-dimensional finite element mesh

which interpolate in terms of unknown point (node) values of the variables. An error, defined as the deviation of the approximation solution from the correct solution, is minimized. Then, when boundary conditions are imposed, a set of solvable simultaneous equations is created. The solution is continuous over the area of interest.

9. In one-dimensional problems, elements are line segments. In two-dimensional problems, the elements are polygons, usually either triangles or quadrilaterals. Nodes are located on the edges of elements and occasionally inside the elements. The interpolating functions may be linear or higher order polynomials. Figure A2 illustrates a quadrilateral element with eight nodes and a linear solution surface where F is the interpolating function.

10. Most water resource applications of the finite element method use the Galerkin method of weighted residuals to minimize error. In this method the residual, the total error between the approximate and correct solutions, is weighted by a function that is identical with the interpolating function and then minimized. Minimization results in a set of simultaneous equations in terms of nodal values of the dependent variable (e.g. water-surface elevations or sediment concentration). The time portion of time-dependent problems can be solved by the finite element method, but it is generally more efficient to express derivatives with respect to time in finite difference form.

The Hydrodynamic Model, RMA-2V

Applications

11. This program is designed for far-field problems in which vertical accelerations are negligible and the velocity vectors at a node generally point in the same directions over the entire depth of the water column at any instant of time. It expects a homogeneous fluid with a free surface. Both steady and unsteady state problems can be analyzed. A surface wind stress can be imposed.

12. The program has been applied to calculate flow distribution around islands; flow at bridges having one or more relief openings, in contracting and expanding reaches, into and out of off-channel hydropower plants, at river junctions, and into and out of pumping plant channels; and general flow patterns in rivers, reservoirs, and estuaries.

Limitations

13. This program is not designed for near-field problems where flow-structure interactions (such as vortices, vibrations, or vertical accelerations) are of interest. Areas of vertically stratified flow are beyond this program's capability unless it is used in a hybrid modeling approach. It is two-dimensional in the horizontal plane, and zones where the bottom current is in a different direction from the surface current must be analyzed with considerable subjective judgment regarding long-term energy considerations. It is a free-surface calculation for subcritical flow problems.

Governing equations

14. The generalized computer program RMA-2V solves the depth-integrated equations of fluid mass and momentum conservation in two horizontal directions. The form of the solved equations is

$$h\frac{\partial u}{\partial t} + hu\frac{\partial u}{\partial x} + hv\frac{\partial u}{\partial y} - \frac{h}{\rho}\left[\epsilon_{xx}\frac{\partial^2 u}{\partial x^2} + \epsilon_{xy}\frac{\partial^2 u}{\partial y^2}\right] + gh\left[\frac{\partial a}{\partial x} + \frac{\partial h}{\partial x}\right]$$

$$+ \frac{gun^2}{\left(1.486h^{1/6}\right)^2}\left[u^2 + v^2\right]^{1/2} - \zeta V_a^2 \cos\psi - 2h\omega v \sin\phi = 0 \qquad \text{(A1)}$$

$$h\frac{\partial v}{\partial t} + hu\frac{\partial v}{\partial x} + hv\frac{\partial v}{\partial y} - \frac{h}{\rho}\left[\epsilon_{yx}\frac{\partial^2 v}{\partial x^2} + \epsilon_{yy}\frac{\partial^2 v}{\partial y^2}\right] + gh\left[\frac{\partial a}{\partial y} + \frac{\partial h}{\partial y}\right]$$

$$+ \frac{gvn^2}{\left(1.486h^{1/6}\right)^2}\left[u^2 + v^2\right]^{1/2} - \zeta V_a^2 \sin\psi + 2\omega hu \sin\phi = 0 \qquad \text{(A2)}$$

$$\frac{\partial h}{\partial t} + h\left[\frac{\partial u}{\partial x} + \frac{\partial v}{\partial y}\right] + u\frac{\partial h}{\partial x} + v\frac{\partial h}{\partial y} = 0 \qquad \text{(A3)}$$

where

h = depth

u,v = velocities in the Cartesian directions

x,y,t = Cartesian coordinates and time

ρ = density

ϵ = eddy viscosity coefficient, for xx = normal direction on x-axis surface; yy = normal direction on y-axis surface; xy and yx = shear direction on each surface

g = acceleration due to gravity

a = elevation of bottom

n = Manning's n value

1.486 = conversion from SI (metric) to non-SI units

ζ = empirical wind shear coefficient

V_a = wind speed

ψ = wind direction

ω = rate of earth's angular rotation

ϕ = local latitude

15. Equations A1, A2, and A3 are solved by the finite element method using Galerkin weighted residuals. The elements may be either quadrilaterals or triangles and may have curved (parabolic) sides. The shape functions are quadratic for flow and linear for depth. Integration in space is performed by Gaussian integration. Derivatives in time are replaced by a nonlinear finite difference approximation. Variables are assumed to vary over each time interval in the form

$$f(t) = f(0) + at + bt^c \qquad t_0 \leq t < t \tag{A4}$$

which is differentiated with respect to time, and cast in finite difference form. Letters a , b , and c are constants. It has been found by experiment that the best value for c is 1.5 (Norton and King 1977).

16. The solution is fully implicit and the set of simultaneous equations is solved by Newton-Raphson iteration. The computer code executes the solution by means of a front-type solver that assembles a portion of the matrix and solves it before assembling the next portion of the matrix. The front solver's efficiency is largely independent of bandwidth and thus does not require as much care in formation of the computational mesh as do traditional solvers.

17. The code RMA-2V is based on the earlier version RMA-2 (Norton and King 1977) but differs from it in several ways. It is formulated in terms of velocity (v) instead of unit discharge (vh), which improves some aspects of the code's behavior; it permits drying and wetting of areas within the grid;

and it permits specification of turbulent exchange coefficients in directions other than along the x- and z-axes. For a more complete description, see Appendix F of Thomas and McAnally (1985).

The Sediment Transport Model, STUDH

Applications

18. STUDH can be applied to clay and/or sand bed sediments where flow velocities can be considered two-dimensional (i.e., the speed and direction can be satisfactorily represented as a depth-averaged velocity). It is useful for both deposition and erosion studies and, to a limited extent, for stream width studies. The program treats two categories of sediment: noncohesive, which is referred to as sand here, and cohesive, which is referred to as clay.

Limitations

19. Both clay and sand may be analyzed, but the model considers a single, effective grain size for each and treats each separately. Fall velocity must be prescribed along with the water-surface elevations, x-velocity, y-velocity, diffusion coefficients, bed density, critical shear stresses for erosion, erosion rate constants, and critical shear stress for deposition.

20. Many applications cannot use long simulation periods because of their computation cost. Study areas should be made as small as possible to avoid an excessive number of elements when dynamic runs are contemplated yet must be large enough to permit proper posing of boundary conditions. The same computation time interval must be satisfactory for both the transverse and longitudinal flow directions.

21. The program does not compute water-surface elevations or velocities; therefore these data must be provided. For complicated geometries, the numerical model for hydrodynamic computations, RMA-2V, is used.

Governing equations

22. The generalized computer program STUDH solves the depth-integrated convection-dispersion equation in two horizontal dimensions for a single sediment constituent. For a more complete description, see Appendix G of Thomas and McAnally (1985). The form of the solved equation is

$$\frac{\partial C}{\partial t} + u\frac{\partial C}{\partial x} + v\frac{\partial C}{\partial y} = \frac{\partial}{\partial x}\left[D_x\frac{\partial C}{\partial x}\right] + \frac{\partial}{\partial y}\left[D_y\frac{\partial C}{\partial y}\right] + \alpha_1 C + \alpha_2 = 0 \qquad \text{(A5)}$$

where

C = concentration of sediment

u = depth-integrated velocity in x-direction

v = depth-integrated velocity in y-direction

D_x = dispersion coefficient in x-direction

D_y = dispersion coefficient in y-direction

α_1 = coefficient of concentration-dependent source/sink term

α_2 = coefficient of source/sink term

23. The source/sink terms in Equation B5 are computed in routines that treat the interaction of the flow and the bed. Separate sections of the code handle computations for clay bed and sand bed problems.

Sand transport

24. The source/sink terms are evaluated by first computing a potential sand transport capacity for the specified flow conditions, comparing that capacity with the amount of sand actually being transported, and then eroding from or depositing to the bed at a rate that would approach the equilibrium value after sufficient elapsed time.

25. The potential sand transport capacity in the model is computed by the method of Ackers and White (1973), which uses a transport power (work rate) approach. It has been shown to provide superior results for transport under steady-flow conditions (White, Milli, and Crabbe 1975) and for combined waves and currents (Swart 1976). Flume tests at the US Army Engineer Waterways Experiment Station have shown that the concept is valid for transport by estuarine currents.

26. The total load transport function of Ackers and White is based upon a dimensionless grain size

$$D_{gr} = D \left[\frac{g(s - 1)}{\nu^2} \right]^{1/3} \tag{A6}$$

where

D = sediment particle diameter

s = specific gravity of the sediment

ν = kinematic viscosity of the fluid

and a sediment mobility parameter

$$F_{gr} = \left[\frac{\tau^{n'}\tau'^{(1-n')}}{\rho g D(s - 1)}\right]^{1/2} \tag{A7}$$

where

τ = total boundary shear stress

n' = a coefficient expressing the relative importance of bed-load and suspended-load transport, given in Equation A9

τ' = boundary surface shear stress

The surface shear stress is that part of the total shear stress which is due to the rough surface of the bed only, i.e., not including that part due to bed forms and geometry. It therefore corresponds to that shear stress that the flow would exert on a plane bed.

27. The total sediment transport is expressed as an effective concentration

$$G_p = C\left[\frac{F_{gr}}{A} - 1\right]^m \frac{sD}{h}\left[\frac{\rho}{\tau} U\right]^{n'} \tag{A8}$$

where U is the average flow speed, and for $1 < D_{gr} \leq 60$

$$n' = 1.00 - 0.56 \log D_{gr} \tag{A9}$$

$$A = \frac{0.23}{\sqrt{D_{gr}}} + 0.14 \tag{A10}$$

$$\log C = 2.86 \log D_{gr} - (\log D_{gr})^2 - 3.53 \tag{A11}$$

$$m = \frac{9.66}{D_{gr}} + 1.34 \tag{A12}$$

For $D_{gr} < 60$

$$n' = 0.00 \tag{A13}$$

$$A = 0.17 \tag{A14}$$

$$C = 0.025 \tag{A15}$$

$$m = 1.5 \tag{A16}$$

28. Equations A6-A16 result in a potential sediment concentration G_p. This value is the depth-averaged concentration of sediment that will occur if an equilibrium transport rate is reached with a nonlimited supply of sediment. The rate of sediment deposition (or erosion) is then computed as

$$R = \frac{G_p - C}{t_c} \tag{A17}$$

where

C = present sediment concentration

t_c = time constant

For deposition, the time constant is

$$t_c = \text{larger of} \begin{cases} \Delta t \\ \text{or} \\ \dfrac{C_d h}{V_s} \end{cases} \tag{A18}$$

and for erosion it is

$$t_c = \text{larger of} \begin{cases} \Delta t \\ \text{or} \\ \dfrac{C_e h}{U} \end{cases} \tag{A19}$$

where

Δt = computational time-step

C_d = response time coefficient for deposition

V_s = sediment settling velocity

C_e = response time coefficient for erosion

The sand bed has a specified initial thickness which limits the amount of erosion to that thickness.

Cohesive sediments transport

29. Cohesive sediments (usually clays and some silts) are considered to be depositional if the bed shear stress exerted by the flow is less than a critical value τ_d. When that value occurs, the deposition rate is given by Krone's (1962) equation

$$S = \begin{cases} -\frac{2V_s}{h} C \left\{1 - \frac{\tau}{\tau_d}\right\} \text{ for } C < C_c & \text{(A20)} \\ -\frac{2V_s}{hC_c^{4/3}} C^{5/3}\left\{1 - \frac{\tau}{\tau_d}\right\} \text{ for } C > C_c & \text{(A21)} \end{cases}$$

where

S = source term

V_s = fall velocity of a sediment particle

h = flow depth

C = sediment concentration in water column

τ = bed shear stress

τ_d = critical shear stress for deposition

C_c = critical concentration = 300 mg/ℓ

30. If the bed shear stress is greater than the critical value for particle erosion τ_e, material is removed from the bed. The source term is then computed by Ariathurai's (Ariathurai, MacArthur, and Krone 1977) adaptation of Partheniades' (1962) findings:

$$S = \frac{P}{h}\left[\frac{\tau}{\tau_e} - 1\right] \text{ for } \tau > \tau_e \qquad \text{(A22)}$$

where P is the erosion rate constant, unless the shear stress is also greater than the critical value for mass erosion. When this value is exceeded, mass failure of a sediment layer occurs and

$$S = \frac{T_L P_L}{h\Delta t} \quad \text{for } \tau > \tau_s \tag{A23}$$

where

T_L = thickness of the failed layer

P_L = density of the failed layer

Δt = time interval over which failure occurs

τ_s = bulk shear strength of the layer

31. The cohesive sediment bed consists of 1 to 10 layers, each with a distinct density and erosion resistance. The layers consolidate with overburden and time.

Bed shear stress

32. Bed shear stresses are calculated from the flow speed according to one of four optional equations: the smooth-wall log velocity profile or Manning equation for flows alone; and a smooth bed or rippled bed equation for combined currents and wind waves. Shear stresses are calculated using the shear velocity concept where

$$\tau_b = \rho u_*^2 \tag{A24}$$

where

τ_b = bed shear stress

u_* = shear velocity

and the shear velocity is calculated by one of four methods:

a. Smooth-wall log velocity profiles

$$\frac{\bar{u}}{u_*} = 5.75 \log \left[3.32 \frac{u_* h}{\nu} \right] \tag{A25}$$

which is applicable to the lower 15 percent of the boundary layer when

$$\frac{u_* h}{\nu} > 30$$

where u is the mean flow velocity (resultant of u and v components)

b. The Manning shear stress equation

$$u_* = \frac{\left(\bar{u}n\right)\sqrt{g}}{CME\ (h)^{1/6}} \tag{A26}$$

where CME is a coefficient of 1 for SI (metric) units and 1.486 for non-SI units of measurement.

c. A Jonsson-type equation for surface shear stress (plane beds) caused by waves and currents

$$u_* = \sqrt{\frac{1}{2}\left[\frac{f_w u_{om} + f_c \bar{u}}{u_{om} + \bar{u}}\right]\left[\bar{u} + u_{om}\right]^2} \tag{A27}$$

where

f_w = shear stress coefficient for waves

u_{om} = maximum orbital velocity of waves

f_c = shear stress coefficient for currents

d. A Bijker-type equation for total shear stress caused by waves and current

$$u_* = \sqrt{\frac{1}{2} f_c \bar{u}^2 + \frac{1}{4} f_w u_{om}^2} \tag{A28}$$

Solution method

33. Equation A5 is solved by the finite element method using Galerkin weighted residuals. Like RMA-2V, which uses the same general solution technique, elements are quadrilateral and may have parabolic sides. Shape functions are quadratic. Integration in space is Gaussian. Time-stepping is performed by a Crank-Nicholson approach with a weighting factor (θ) of 0.66. A front-type solver similar to that in RMA-2V is used to solve the simultaneous equations.

References

Ackers, P., and White, W. R. 1973. (Nov). "Sediment Transport: New Approach and Analysis," Journal, Hydraulics Division, American Society of Civil Engineers, Vol 99, No. HY-11, pp 2041-2060.

Ariathurai, R., MacArthur, R. D., and Krone, R. C. 1977 (Oct). "Mathematical Model of Estuarial Sediment Transport," Technical Report D-77-12, US Army Engineer Waterways Experiment Station, Vicksburg, MS.

Krone, R. B. 1962. "Flume Studies of Transport of Sediment in Estuarial Shoaling Processes," Final Report, Hydraulics Engineering Research Laboratory, University of California, Berkeley, CA.

Norton, W. R., and King, I. P. 1977 (Feb). "Operating Instructions for the Computer Program RMA-2V," Resource Management Associates, Lafayette, CA.

Partheniades, E. 1962. "A Study of Erosion and Deposition of Cohesive Soils in Salt Water," Ph.D. Dissertation, University of California, Berkeley, CA.

Swart, D. H. 1976 (Sep). "Coastal Sediment Transport, Computation of Longshore Transport," R968, Part 1, Delft Hydraulics Laboratory, The Netherlands.

Thomas, W. A., and McAnally, W. H., Jr. 1985 (Aug). "User's Manual for the Generalized Computer Program System; Open-Channel Flow and Sedimentation, TABS-2, Main Text and Appendices A through O," Instruction Report HL-85-1, US Army Engineer Waterways Experiment Station, Vicksburg, MS.

White, W. R., Milli, H., and Crabbe, A. D. 1975. "Sediment Transport Theories: An Appraisal of Available Methods," Report Int 119, Vols 1 and 2, Hydraulics Research Station, Wallingford, England.